Superacid Anions: Crystal and Molecular Structures of Oxonium Undecafluorodiantimonate(V), $[H_3O][Sb_2F_{11}]$, Cesium Fluorosulfate, $CsSO_3F$, Cesium Hydrogen Bis(fluorosulfate), $Cs[H(SO_3F)_2]$, Cesium Tetrakis(fluorosulfato)aurate(III), $Cs[Au(SO_3F)_4]$, Cesium Hexakis(fluorosulfato)platinate(IV), $Cs_2[Pt(SO_3F)_6]$, and Cesium Hexakis(fluorosulfato)antimonate(V), $Cs[Sb(SO_3F)_6]$

Dingliang Zhang, Steven J. Rettig, James Trotter, and Friedhelm Aubke*

Department of Chemistry, The University of British Columbia, Vancouver, BC, Canada V6T 1Z1

Received May 10, 1996[⊗]

In order to understand the reasons for the low nucleophilicity of superacid anions, a systematic, comparative study of six superacid anions by single-crystal X-ray diffraction is undertaken. From magic acid, HSO_3F-SbF_5, surprisingly, single crystals of oxonium undecafluorodiantimonate(V), $[H_3O][Sb_2F_{11}]$, **1**, are obtained. In the remaining five salts the cesium ion, Cs^+, is used as the countercation. Both $CsSO_3F$, **2**, and its solvate $Cs[H(SO_3F)_2]$, **3**, are derived from the Brönsted superacid HSO_3F. The conjugate noble metal superacid systems $HSO_3F-Au(SO_3F)_3$ and $HSO_3F-Pt(SO_3F)_4$ provide cesium tetrakis(fluorosulfato)aurate(III) $Cs[Au(SO_3F)_4]$, **4**, and cesium hexakis(fluorosulfato)platinate(IV) $Cs_2[Pt(SO_3F)_6]$, **5**. Cesium hexakis(fluorosulfato)antimonate(V) $Cs[Sb(SO_3F)_6]$, **6**, whose synthesis is described here in detail, provides evidence for the possible existence of a new conjugate superacid system, $HSO_3F-Sb(SO_3F)_5$. Crystals of $[H_3O][Sb_2F_{11}]$ (**1**, $H_3F_{11}OSb_2$) are orthorhombic, $a = 12.744(2)$ Å, $b = 39.371(2)$ Å, $c = 11.407(3)$ Å, $Z = 24$, and space group *Pbca*; those of $CsSO_3F$ (**2**, $CsFO_3S$) are monoclinic, $a = 7.7243(6)$ Å, $b = 8.1454(6)$ Å, $c = 7.7839(7)$ Å, $\beta = 110.832(7)°$, $Z = 4$, and space group $P2_1/a$; those of $Cs[H(SO_3F)_2]$ (**3**, $HCsF_2O_6S_2$) are monoclinic, $a = 13.371(2)$ Å, $b = 7.731(2)$ Å, $c = 9.485(2)$ Å, $\beta = 128.375(7)°$, $Z = 4$, and space group $C2/c$; those of $Cs[Au(SO_3F)_4]$ (**4**, $AuCsF_4O_{12}S_4$) are monoclinic, $a = 17.725(2)$ Å, $b = 5.822(2)$ Å, $c = 14.624(2)$ Å, $\beta = 102.120(9)°$, $Z = 4$, and space group $C2/c$; those of $Cs_2[Pt(SO_3F)_6]$ (**5**, $Cs_2F_6O_{18}PtS_6$) are trigonal, $a = 9.070(1)$ Å, $c = 7.6028(7)$ Å, $Z = 1$, space group $P321$; and those of $Cs[Sb(SO_3F)_6]$ (**6**, $CsF_6O_{18}S_6Sb$) are trigonal, $a = 12.0317(7)$ Å, $c = 12.026(2)$ Å, $Z = 3$, space group $R\bar{3}$. The structures were solved by Patterson (**1**, **2**, and **6**) or direct (**4** and **5**) methods (that of **3** is a redetermination) and were refined by full-matrix least-squares procedures to $R = 0.036$, 0.029, 0.027, 0.030, 0.048, and 0.039 ($R_w = 0.032$, 0.027, 0.026, 0.029, 0.045, and 0.037) for 4110, 2321, 1362, 1671, 738, and 1485 reflections with $I \geq 3\sigma(F^2)$, for **1**, **2**, **3**, **4**, **5**, and **6**, respectively. In addition $Cs[Sb(SO_3F)_6]$ is characterized by vibrational spectroscopy.

Introduction

Superacids[1,2] are used as reaction media for the generation, stabilization, and synthetic application of highly electrophilic and frequently very reactive organic,[2] inorganic,[1,3] and selected metalorganic[4] cations. As is evident from the autoprotolysis equilibria for a Brönsted superacid[1,2] like HSO_3F,[1,5] the protonic acid of choice in this study

$$2HSO_3F \rightleftarrows H_2SO_3F^+(solv) + SO_3F^-(solv) \qquad (1)$$

or for a conjugate superacid in fluorosulfuric acid, the HSO_3F-$Au(SO_3F)_3$ system[6]

$$2HSO_3F + Au(SO_3F)_3 \rightleftarrows H_2SO_3F^+(solv) + [Au(SO_3F)_4]^-(solv) \qquad (2)$$

the usefulness of superacid media is determined by three interrelated general properties of the solvent system and its constituent ions: (a) **the proton donor strength** or **proton acidity**, which should be very high, but is limited in the above examples by the proton donor strength of the acidium ion, $H_2SO_3F^+$(solv); (b) the **nucleophilicity** or **electron pair donor ability** of the base, or the conjugate base ion, SO_3F^-(solv) or $[Au(SO_3F)_4]^-$(solv), respectively, which should be very low, and (c) in case of conjugate superacids, the **electron pair acceptor strength** or **Lewis acidity** of the molecular Lewis acid, in our example $Au(SO_3F)_3$.

It has in the past been possible to measure or estimate the proton donor strength of both Brönsted and conjugate superacids. Hammet acidity function values $-H_o$[7a] have become known for many systems[2,8] and electrochemical methods[7b] have yielded a comparable scale of $R_o(H)$ values,[2,9] which in turn have also allowed relative rankings of various molecular Lewis acids.[2,9] A critical assessment of the various methods to estimate the acidity of superacids has appeared recently.[10]

⊗ Abstract published in *Advance ACS Abstracts,* September 15, 1996.

(1) Gillespie, R. J. *Acc. Chem. Res.* **1968**, *1*, 202.
(2) Olah, G. A.; Prakash, G. K. S.; Sommer, L. "*Superacids*", Wiley, New York, 1985, and references therein.
(3) O'Donnell, T. A. *Superacids and Acidic Melts as Inorganic Chemical Reaction Media*; VCH Publishers: New York, 1993 and references therein.
(4) Aubke, F.; Wang; C. *Coord. Chem. Rev.* **1994**, *137*, 483.
(5) Thompson, R. C. In *Inorganic Sulphur Chemistry*; Nickless, G., Ed.; Elsevier: Amsterdam, 1968; p 587.
(6) (a) Lee, K. C.; Aubke, F. *Inorg. Chem.* **1979**, *18*, 389. (b) Lee, K. C.; Aubke, F. *Inorg. Chem.* **1980**, *19*, 119.
(7) (a) Hammet, L. P.; Deyrup, A. J. *J. Am. Chem. Soc.* **1932**, *54*, 2721. (b) Strehlow, H.; Wendt, H. *Phys. Chem. (Frankfurt)* **1960**, *30*, 141.
(8) Gillespie, R. J.; Peel, T. E. *Adv. Phys. Org. Chem.* **1972**, *9*, 1.
(9) Fabré, P. L.; Devynck, J.; Tremillon, B. *Chem. Rev.* **1982**, *82*, 591.

S0020-1669(96)00525-3 CCC: $12.00

It has been far more difficult to estimate the nucleophilicity of the Brönsted or conjugate superacid anions in solution or in solid compounds. A ranking based on ^{119}Sn Mössbauer parameters (the isomer shift δ and the quadrupole splitting ΔE_Q) for $(CH_3)_2Sn^{2+}$ derivatives of protonic acids and superacids[11] is obviously limited to those acids that form dimethyltin(IV) salts with linear C−Sn−C skeletal groups. Where this group becomes nonlinear as e.g., in a number of dimethyltin(IV) carboxylates,[12] the resulting asymmetry around tin reduces ΔE_Q,[13] and the suggested correlation with anion nucleophilicity fails.[11]

The approach pursued in this study is based on the observation that many acid anions and some superacid anions form isolable salts with simple cations, which may then be structurally characterized by single-crystal X-ray diffraction. The cesium cation, Cs^+, is chosen for three reasons: (i) Cs^+ has the lowest ionic potential of the alkali metal cations and it should be the least electrophilic and polarizing ion among univalent monoatomic cations. (ii) Cs^+ is obviously reductively and oxidatively stable and its salts are highly soluble in many strong acids or superacids. (iii) Many Cs^+ salts with superacid anions are known and are frequently characterized by vibrational spectroscopy. In one instance, that of $Cs[H(SO_3F)_2]$,[14] a preliminary molecular structure determination exists, but only the O−H−O distance is reported and a very strong, symmetrical hydrogen bond is suggested.

We have very recently been successful in obtaining single crystals, suitable for structure determinations on polymeric materials of the type $[SbF_n(SO_3F)_{3-n}]_x$, $n = 0$, 1 or 2, by recrystallization from fluorosulfuric acid, HSO_3F.[15] This procedure is now applied in order to obtain single crystals of a number of cesium salts with superacid anions and we report here their molecular structures.

In all instances, previously reported synthetic procedures are employed. $CsSO_3F$[16] and the monosolvate $Cs[H(SO_3F)_2]$[14,17] are derived from the Brönsted superacid HSO_3F. From the noble metal conjugate superacid systems $HSO_3F-Au(SO_3F)_3$[6] and $HSO_3F-Pt(SO_3F)_4$,[18] the salts $Cs[Au(SO_3F)_4]$[6] and $Cs_2[Pt(SO_3F)_6]$[18] are obtained. We have also been able to grow single crystals of $Cs_2[Sn(SO_3F)_6]$[19,20] and have obtained diffraction data, but it has so far not been possible to solve the crystal structure of this material.

When the general route to synthesize $Cs[Au(SO_3F)_4]$,[6] $Cs_2[Pt(SO_3F)_6]$,[18] and $Cs_2[Sn(SO_3F)_6]$,[20] the metal oxidation by bis(fluorosulfuryl) peroxide[21] in the presence of stoichiometric amounts of $CsSO_3F$ and in HSO_3F as solvent, is adapted to the oxidation of antimony, the salt $Cs[Sb(SO_3F)_6]$ is obtained. Again recrystallization from HSO_3F affords single crystals. The subsequent structure determination is described in a preliminary account.[22] We report here full details on the synthesis and the characterization of $Cs[Sb(SO_3F)_6]$ by its vibrational spectra compared to those of $Cs_2[Pt(SO_3F)_8]$[8] and $Cs[Au(SO_3F)_4]$.[6] The conjugate superacid system $HSO_3F-Sb(SO_3F)_5$ is presently unknown. Detailed studies of the ternary system $HSO_3F-SO_3-SbF_5$[23] have revealed that the highest acidity is observed at a SO_3 to SbF_5 ratio of 3:1, which would suggest an anion of the composition $[SbF_2(SO_3F)_4]^-$. It has not been possible to isolate crystalline salts with this anion. As ^{19}F-NMR studies on this[23] and the related conjugate superacid HSO_3F-SbF_5[24,25] indicate, F vs SO_3F exchange, solute (SbF_5) solvolysis, and concentration dependent anion association via SO_3F or F bridges are responsible for complex equilibria involving several anionic species.[23]

It is therefore surprising that single crystals are obtained from magic acid solutions of 30−50 mol % of SbF_5 in HSO_3F after several weeks, with the solutions contained in glass NMR tubes. The molecular structure determination and Raman spectra allow identification of the material as $[H_3O][Sb_2F_{11}]$. Since the oxonium ion H_3O^+ is very well characterized and the molecular structure of $[H_3O][SbF_6]$ is known,[26,27] the structural analysis of $[H_3O][Sb_2F_{11}]$ will concentrate on the anion $[Sb_2F_{11}]^-$ and the distortions of the anion induced by various OH--F hydrogen bond types. The complex structure of $[H_3O][Sb_2F_{11}]$ reveals three crystallographically different $[Sb_2F_{11}]^-$ ions, due to various types of interionic linkage via weak, asymmetric hydrogen bonds of the O−H--F type.

As in the case of $[H_3O][Sb_2F_{11}]$ and $[H_3O][SbF_6]$,[26,27] there are related precedents for the remaining five structures reported here. Among simple ionic fluorosulfates, the structures of the Li^+,[28] K^+,[29] and NH_4^+ [30] salts are known. However the anion SO_3F^- is highly distorted from C_{3v} symmetry in the lithium salt on account of the strongly polarizing Li^+ cation.[28] In both KSO_3F[29] NH_4SO_3F[30] the fluorosulfate anion is disordered. For $CsSO_3F$, the space group $I4_1/a$ has been determined in an early study,[31] which is however at variance with our findings presented below but probably corresponds to a different crystal form.

There are also many examples of strong, symmetrical hydrogen bonds[32] of the O−H−O type as e.g. in the $[H(OTeF_5)_2]^-$ ion;[33] however the hydrogen bond in $[H(SO_3F)_2]^-$ appears to be one of the shortest and strongest of this bond type.[14]

An analogous anion to $[Au(SO_3F)_4]^-$ is found in the salt $K[Au(NO_3)_4]$, which is structurally characterized.[34] In addition the molecular structure of $[Au(SO_3F)_3]_2$, the Lewis acid in the

(10) Jost, R.; Sommer, J. *Rev. Chem. Intermed.* **1988**, *9*, 1.
(11) Mallela, S. P.; Yap, S.; Sams, J. R.; Aubke, F. *Inorg. Chem.* **1986**, *25*, 4327.
(12) Mistry, F.; Rettig, S. J.; Trotter, J.; Aubke, F. *Z. Anorg. Allg. Chem.* **1995**, *621*, 1875.
(13) Bancroft, G. M.; Platt, R. H. *Adv. Inorg. Chem. Radiochem.* **1972**, *15*, 59.
(14) Belin, C.; Charbónnel, M.; Potier, J. *J. Chem. Soc., Chem. Commun.* **1981**, 1036.
(15) Zhang, D.; Rettig, S. J.; Trotter, J.; Aubke, F.; *Inorg. Chem.* **1995**, *34*, 3153.
(16) (a) Lange, W. *Chem. Bev.* **1927**, *60*, 962. (b) Barr, J.; Gillespie, R. J.; Thompson, R. C. *Inorg. Chem.* **1964**, *3*, 1149. (c) Ruoff, A.; Milne, J. B.; Kaufmann, G.; Leroy, M. *Z. Anorg. Allg. Chem.* **1970**, *372*, 119.
(17) Josson, C.; Deporco-Stratmains, M.; Vast, P. *Bull Soc. Chim. Fr.* **1977**, 820.
(18) Lee, K. C.; Aubke, F. *Inorg. Chem.* **1984**, *23*, 2124.
(19) Yeats, P. A.; Sams, J. R.; Aubke, F. *Inorg. Chem.* **1973**, *12*, 328.
(20) Mallela, S. P.; Lee, K. C.; Aubke, F. *Inorg. Chem.* **1984**, *23*, 653.
(21) Dudley, F. B.; Cady, G. H. *J. Am. Chem. Soc.* **1957**, *79*, 513.
(22) Zhang, D.; Rettig, S. J.; Trotter, J.; Aubke, F. *Inorg. Chem.* **1995**, *34*, 2269.
(23) (a) Thompson, R. C.; Barr, J.; Gillespie, R. J.; Rothenbury, R. A. *Inorg. Chem.* **1965**, *4*, 1641. (b) Zhang, D.; Heubes, M.; Hägele, G.; Aubke, F. *Inorg. Chem.*, to be submitted for publication.
(24) Dean, P. A. W.; Gillespie, R. J. *J. Am. Chem. Soc.* **1970**, *92*, 2362.
(25) (a) Olah, G. A.; Commeyras, A. *J. Am. Chem. Soc.* **1969**, *91*, 2929. (b) Brunet, D.; Germain, A.; Commeyras, A. *Nouv. J. Chim.* **1978**, *2*, 275.
(26) Christe, K. O.; Charpin, P.; Soulie, E.; Bougon, R.; Fawcett, J.; Russell, D. R. *Inorg. Chem.* **1984**, *23*, 3756.
(27) Larson, E. M.; Abney, K. D.; Larson, A. C.; Eller, P. G. *Acta Crystallogr.* **1991**, *B47*, 206.
(28) Zák, Z.; Kosicka, M. *Acta Crystallogr.* **1978**, *B34*, 38.
(29) O'Sullivan, K.; Thompson, R. C.; Trotter, J. *J. Chem. Soc. A* **1967**, 202.
(30) O'Sullivan, K.; Thompson, R. C.; Trotter, J. *J. Chem. Soc. A* **1970**, 1814.
(31) Seifert, H. *Z. Kristallogr. Mineralog. Petrogr.* **1942**, *104*, 1385.
(32) Emsley, J. *Chem. Soc. Rev.* **1980**, *9*, 91.
(33) Strauss, S. H.; Abney, K. D.; Anderson, O. P. *Inorg. Chem.* **1986**, *25*, 2806 and references therein.
(34) Garner, C. D.; Wallwork, S. C. *J. Chem. Soc. A* **1970**, 309.

conjugate superacid $HSO_3F-Au(SO_3F)_3$, is known[35] and should allow a structural comparison to $[Au(SO_3F)_4]^-$.

Finally, the molecular structures of salts of the composition $[N(CH_3)_4][E(OTeF_5)_6]$, E = As, Sb, or Bi, have recently been reported.[36] The structures of the anions in these salts allow comparisons to $[Sb(SO_3F)_6]^-$ as weakly coordinating anions. Such large, weakly coordinating anions are of current interest.[37] Our work on carbonyl cations of electron-rich metals[4,38] has pointed to another useful property such anions must possess. Starting with the observation that almost all thermally stable salts in this group have $[Sb_2F_{11}]^-$ as counteranion, while the vast majority of the cationic carbonyl derivatives are fluorosulfates, we have undertaken structural studies on *cis*-$Pd(CO)_2(SO_3F)_2$,[39] $[Hg(CO)_2][Sb_2F_{11}]_2$,[40] *mer*-$Ir(CO)_3(SO_3F)_3$,[41] and $[Ir(CO)_5Cl][Sb_2F_{11}]_2$.[42] The structures have indicated, that in the absence of substantial metal ion to carbon π-back-bonding, significant inter- and intramolecular[39,41] or interionic contacts[40] between F or O atoms of the anion[40] or the anionic group[39,41] are observed and appear to stabilize the structures in the solid state. Similar weak interactions to those observed in $[Hg(CO)_2][Sb_2F_{11}]_2$[40] are found for $[H_3O][Sb_2F_{11}]$ and are discussed below. Here the protons of the $[H_3O]^+$ cation take the place of the electrophilic C atom in the $[Hg(CO)_2]^{2+}$ salt. In the cesium salts similar weak interionic contacts are observed in the coordination sphere of the Cs^+ ion (vide infra).

In summary, attention in this study will concentrate on two aspects: (a) strong covalent bonding within the superacid anions as a manifestation of their low nucleophilicity and (b) their involvement in weak interionic interactions with either H_3O^+ or Cs^+ as an indication of the anion's ability to stabilize other highly electrophilic, molecular cations by weak secondary interionic interactions.

Experimental Section

(a) Chemicals. Antimony metal powder (Sb, 99.5% pure, 100 mesh) was obtained from Matheson Coleman and Bell. Both gold powder (99.995% pure, 20 mesh) and platinum powder (99.9% pure 0.27−0.4 micron) were obtained from Johnson Matthey Electronics. Cesium chloride (CsCl, A.R.) was purchased from BDH Chemicals. Antimony pentafluoride (SbF_5, 99% pure) was obtained from Ozark-Mahoning (now known as Atochem North America). It was first distilled using a regular distillation apparatus under flow of dry nitrogen at atmospheric pressure and then trap to trap distilled *in vacuo*. $S_2O_6F_2$ was obtained by the catalytic fluorination of SO_3 over AgF_2.[43] Technical grade fluorosulfuric acid HSO_3F (Orange County Chemicals, Anaheim, CA) was purified by double-distillation in a counterflow of dry N_2 under atmospheric pressure as described previously.[6b] $CsSO_3F$,[16a,16c] $Cs[H(SO_3F)_2]$,[14] $Cs[Au(SO_3F)_4]$,[6] and $Cs_2[Pt(SO_3F)_6]$[18] are prepared as reported previously.

(b) Equipment and Instrumentation. Standard vacuum-line techniques were employed to manipulate moisture-sensitive samples. A Vacuum Atmosphere Corporation DRI-LAB Model Dl-001-S-G dry box, filled with dry nitrogen and equipped with an HE 493 Dri-Train, was also used to manipulate and store moisture sensitive, nonvolatile solids and liquids. Reactions were carried out in Pyrex tubular reactors with a sidearm of the approximate shape of an inverted Y. The reactor was fitted with a Kontes Teflon stopcock, and a magnetic stirring bar was inserted in the main arm of the reactor.

Infrared spectra down to 300 cm^{-1} were recorded on a Bomem MB-102 FT-IR spectrometer. Solid samples were finely ground and pressed as thin films between AgBr windows (Harshaw Chemicals). Raman spectra were recorded with a Bruker RFS 100 FT-Raman accessory, mounted on an optical bench of a Bruker IFS-66v FT-IR instrument. Solid samples were ground and loaded inside a drybox into a melting point capillary tube, which was subsequently flame-sealed. ^{19}F NMR spectra were recorded on a Varian XL-300 multinuclear spectrometer. A solution of 5% $CFCl_3$ (reference) in acetone-d_6 (lock solvent) was sealed in capillary tubes, which were inserted coaxially in the NMR tubes, supported by two Teflon spacers. The solution samples were loaded into 50 mm o.d. NMR tubes inside the drybox and flame-sealed under vacuum.

(c) Preparations of Single Crystals of $[H_3O][Sb_2F_{11}]$, 1. During the course of NMR studies of the conjugate superacid HSO_3F-SbF_5 system, colorless crystals were precipitated after long standing at room temperature from the sealed NMR samples contained in glass tubes of high SbF_5 content ($\geq$30 mol %). The sealed NMR tubes were cut open inside the drybox. A colorless, prism crystal with approximate size of 0.30 × 0.30 × 0.35 mm was carefully separated from the mixture and loaded into a 0.5 mm *Mark*-capillary tube.

$CsSO_3F$, 2, and $Cs[H(SO_3F)_2]$, 3. $Cs[H(SO_3F)_2]$ was obtained by solvolysis of CsCl in excess of HSO_3F.[14,17] Crystals were grown by allowing the hot, saturated solution to cool slowly to room temperature. The crystals were separated from the supernatant by filtration inside a drybox. The single crystals for an X-ray diffraction study were loaded into a Lindemann glass capillary tube without any further drying procedure. A Raman spectrum was obtained from the crystals after pumping at room temperature for 24 h as a purity check. Crude $CsSO_3F$ powder was obtained by heating $Cs[H(SO_3F)_2]$ *in vacuo* to 120 °C for 3 days. Single crystals were obtained by recrystallization of $CsSO_3F$ from deionized water.

$Cs[Au(SO_3F)_4]$, 4, and $Cs_2[Pt(SO_3F)_6]$, 5. The compounds $Cs[Au(SO_3F)_4]$ and $Cs_2[Pt(SO_3F)_6]$ were synthesized by metal oxidation with $S_2O_6F_2$[42] in HSO_3F in the presence of stoichiometric amounts of $CsSO_3F$.[6,18] $CsSO_3F$ was prepared in situ prior to the oxidation reaction from CsCl in HSO_3F solution as discussed above. Single crystals of $Cs_2[Pt(SO_3F)_6]$ were grown by allowing a hot, saturated solution in HSO_3F to cool slowly to room temperature, while single crystals of $Cs[Au(SO_3F)_4]$ were obtained from a solution in HSO_3F by controlled removal of the solvent *in vacuo*.

Preparation of $Cs[Sb(SO_3F)_6]$, 6. In a typical reaction, 0.169 g (1.00 mmol) of CsCl was placed in the side arm of the reactor. About 10.5 g HSO_3F (105 mmol) was pipetted into the main tubular side arm of the reactor inside the drybox. HSO_3F was mixed with CsCl to allow the reaction to proceed. After all CsCl had dissolved, the solution was stirred at room temperature for about an hour. During the reaction, HCl produced in the reaction was removed intermittently. The solution was then maintained in a dynamic vacuum to remove all HCl. A slight loss of HSO_3F at this stage was noted.

(35) Willner, H.; Rettig, S. J.; Trotter, J.; Aubke, F. *Can. J. Chem.* **1991**, *69*, 391.
(36) Mercier, H. P. A.; Sanders, J. C. P.; Schrobilgen, G. J. *J. Am. Chem. Soc.* **1994**, *116*, 2921.
(37) Strauss, S. H. *Chem. Rev.* **1993**, *93*, 927.
(38) Aubke, F. *J. Fluorine Chem.* **1995**, *72*, 195.
(39) Wang, C.; Willner, H.; Bodenbinder, M.: Batchelor, R. J.; Einstein, F. W. B.; Aubke, F. *Inorg. Chem.* **1994**, *33*, 3521.
(40) Bodenbinder, M.; Balzer-Jöllenbeck, G.; Willner, H.; Batchelor, R. J.; Einstein, F. W. B.; Wang, C.; Aubke, F. *Inorg. Chem.* **1996**, *35*, 82.
(41) Wang, C.; Lewis, A. R.; Batchelor, R. J.; Einstein, F. W. B.; Willner, H.; Aubke, F. *Inorg. Chem.* **1996**, *35*, 1279.
(42) Bach, C.; Wang, C.; Rettig, S. J.; Trotter, J.; Willner, H.; Aubke, F. *Angew. Chem.* **1996**, *108*, 2104.
(43) (a) Cady, G. H.; Shreeve, J. M. *Inorg. Synth.* **1963**, *7*, 124. (b) Zhang, D.; Wang, C.; Mistry, F.; Powell, B.; Aubke, F. *J. Fluorine Chem.* **1996**, *76*, 83.

Table 1. Crystallographic Data[a]

	$[H_3O][Sb_2F_{11}]$, **1**	$Cs(SO_3F)$, **2**	$Cs[H(SO_3F)_2]$, **3**	$Cs[Au(SO_3F)_4]$, **4**	$Cs_2[Pt(SO_3F)_6]$, **5**	$Cs[Sb(SO_3F)_6]$, **6**
formula	$H_3F_{11}OSb_2$	$CsFO_3S$	$HCsF_2O_6S_2$	$AuCsF_4O_{12}S_4$	$Cs_2F_6O_{18}PtS_6$	$CsF_6O_{18}S_6Sb$
fw	471.51	231.96	332.63	726.10	1055.24	848.99
cryst syst	orthorhombic	monoclinic	monoclinic	monoclinic	trigonal	trigonal
space group	Pbca	$P2_1/a$	$C2/c$	$C2/c$	$P321$	$R\bar{3}$
a, Å	12.744(2)	7.7243(6)	13.371(2)	17.725(2)	9.070(1)	12.0317(7)
b, Å	39.371(2)	8.1454(6)	7.731(2)	5.822(2)	9.070(1)	12.0317(7)
c, Å	11.407(3)	7.7839(7)	9.485(2)	14.624(2)	7.6028(7)	12.026(2)
β, deg		110.832(7)	128.375(7)	102.120(9)		
V, Å^3	5723(1)	457.72(7)	768.6(3)	1475.5(5)	541.64(6)	1507.6(2)
Z	24	4	4	4	1	3
D_{calc}, g/cm^3	3.283	3.366	2.869	3.268	3.235	2.805
T, °C	21	21	21	21	21	21
λ, Å	0.710 69	0.710 69	0.710 69	0.710 69	0.710 69	0.710 69
μ(Mo Kα), cm^{-1}	57.95	84.44	53.83	131.03	104.69	39.15
R	0.036	0.029	0.027	0.030	0.048	0.039
R_w	0.032	0.027	0.026	0.029	0.045	0.037

[a] $R = \sum(|F_o| - |F_c|)/\sum|F_o|$, $R_w = [\sum w(|F_o| - |F_c|)^2/\sum w|F_o|^2]^{1/2}$.

Subsequently, the solution was collected into the main arm of the reactor. Antimony powder (0.1206 g, 0.991 mmol) was added to the side arm side of the reactor inside the drybox. Then 1.30 mL (2.24 g, 11.3 mmol) of $S_2O_6F_2$, premeasured in a pipette fitted with a Kontes Teflon stopcock, was transferred into the reactor in vacuo and condensed onto the main side of the reactor. The solution was then mixed with antimony metal and stirred at 70 °C overnight. All metal was consumed within 12 h to give a colorless solution. By removal of volatiles and HSO_3F in vacuo, the volume of the solution was reduced to about 3 mL. At this point, a colorless, crystalline solid appeared in the solution. Complete removal of the solvent yielded a product with a red-orange color.

To purify the compound, the raw product was dissolved in about 3 mL of HSO_3F at 50 °C. The solution was then controlled to cool down very slowly to room temperature. The colorless, cube-shaped single crystals suitable for X-ray diffraction analysis were obtained after filtration in vacuo.

Characterization of $Cs[Sb(SO_3F)_6]$. The colorless, hygroscopic crystals decomposed when heated in a sealed tube at 149 °C to give a brown residue. The composition was established by the mass balance of the reaction.

X-ray Crystallographic Analyses. Crystallographic data appear in Table 1. The following labeling of the six compounds studied here was adopted. $[H_3O][Sb_2F_{11}]$, **1**, $CsSO_3F$, **2**, $Cs[H(SO_3F)_2]$, **3**, $Cs[Au(SO_3F)_4]$, **4**, $Cs_2[Pt(SO_3F)_6]$, **5**, and $Cs[Sb(SO_3F)_6]$, **6**. The final unit-cell parameters were obtained by least-squares on the setting angles for 25 reflections with $2\theta = 29.2-32.4°$ for **1**, 52.9−58.6° for **2**, and 42.9−48.1° for **3**, 31.1−41.5° for **4**, 31.8−40.2° for **5**, and 42.1−44.6° for **6**. The intensities of three standard reflections, measured every 200 reflections throughout the data collections, decreased uniformly by 3.2% for **1** and by 11.5% for **3**, and showed only small random fluctuations for **2**, **4**, **5**, and **6**. The data were processed,[44] corrected for Lorentz and polarization effects, decay (for **1** and **3**), and absorption (empirical, based on azimuthal scans for three reflections).

The structures of **1**, **2**, and **6** were determined by the Patterson method and those of **4** and **5** were determined by direct methods. The asymmetric unit of **1** contains three formula units. The unit cell originally reported for **3**[14] can be transformed to that used here by the matrix $(\bar{1}00/0\bar{1}0/101)$. As previously reported, the Cs^+ ion in **3** lies on a crystallographic 2-fold axis. In **4** the Au atom lies on a center of symmetry and the Cs^+ ion lies on a 2-fold axis. One of the fluorosulfate ligands in **4** was refined as 2-fold disordered, with the S and F atoms disordered by reflection (approximately) across the O_3 plane. Atoms O(5) and O(6) were probably disordered as well, but could not be satisfactorily modeled. As a result, the geometrical parameters of the fluorosulfate showed deviations from expected values. The population parameter of the higher occupancy S atom (S(2)) was refined and the populations of the remaining disordered atoms were constrained accordingly. Compound **5** may have a superlattice structure with $c' = 2c$. A superlattice data set was collected but attempts to solve the structure were unsuccessful. The l odd data were generally very weak with less than 4% having significant intensity. The structure analysis of **5** was thus undertaken in the small unit cell reported here. There are three possible space groups for **5**: $P\bar{3}m1$, $P3m1$, or $P321$. The structure analysis was first attempted, unsuccessfully, in the centrosymmetric space group ($P\bar{3}m1$) on the basis of the E-statistics. Subsequent attempts in the noncentrosymmetric space groups eventually led to a reasonable result in space group $P321$. The anion in **5** has crystallographic 32 (D_3) symmetry and the Cs^+ ion has crystallographic 3 (C_3) symmetry. In **6**, both Sb and Cs atoms are located at lattice points having S_6 symmetry.

All non-hydrogen atoms were refined with anisotropic thermal parameters. The hydrogen atom positions of **1** were idealized from difference map positions (O−H = 0.89 Å, $B_H = 1.2B_{\text{bonded atom}}$). The proton in **3** (the largest difference map peak after anisotropic refinement of the non-hydrogen atoms) lies on a crystallographic center of symmetry. The isotropic thermal parameter of this H atom was refined. Corrections for secondary extinction (Zachariasen type II, isotropic) were applied for five of the structures, the final values of the extinction coefficients being $1.17(13) \times 10^{-8}$ for **1**, $1.39(2) \times 10^{-6}$ for **2**, $4.09(6) \times 10^{-6}$ for **3**, $5.90(11) \times 10^{-7}$ for **4**, and $1.93(3) \times 10^{-6}$ for **6**. No extinction correction was necessary for **5**. Neutral atom scattering factors for all atoms and anomalous dispersion corrections for the non-hydrogen atoms were taken from refs 45 and 46. A parallel refinement of the mirror-image structure of **5** gave significantly higher residuals, the R and R_w factor ratios both being 1.06.

Final atomic coordinates and equivalent isotropic thermal parameters, bond lengths, and bond angles appear in Tables 2−4, respectively. Complete tables of crystallographic data, anisotropic thermal parameters, torsion angles, and intermo-

(44) *teXsan: Crystal Structure Analysis Package*; Molecular Structure Corporation: The Woodlands, TX, 1985 and 1992.

(45) *International Tables for X-ray Crystallography*; Kynoch Press: Birmingham, England, 1974; Vol. IV, pp 99−102

(46) *International Tables for Crystallography*; Kluwer Academic Publishers: Boston, MA, 1992; Vol. C, pp 200−206.

Table 2. Atomic Coordinates and Equivalent Isotropic Thermal Parameters[a]

atom	x	y	z	B_{eq}/B_{iso}, Å^2	atom	x	y	z	B_{eq}/B_{iso}, Å^2
				$[H_3O][Sb_2F_{11}]$, **1**					
Sb(1)	0.46438(4)	0.05248(1)	0.13656(5)	3.86(1)	F(21)	0.7791(5)	0.2279(2)	−0.0939(6)	8.4(2)
Sb(2)	0.20221(5)	0.01976(2)	0.00068(6)	4.71(2)	F(22)	0.5886(5)	0.2463(2)	−0.1289(6)	9.8(2)
Sb(3)	0.50719(4)	0.18277(1)	0.10926(6)	3.77(1)	F(23)	0.2596(3)	0.1349(1)	0.6020(4)	4.9(1)
Sb(4)	0.68504(5)	0.25490(2)	−0.01397(6)	4.35(1)	F(24)	0.4932(4)	0.1233(1)	0.3883(5)	6.2(2)
Sb(5)	0.38055(4)	0.12917(2)	0.48880(5)	3.85(1)	F(25)	0.3349(6)	0.1685(2)	0.4216(7)	11.0(3)
Sb(6)	0.21358(5)	0.13366(2)	0.77216(5)	4.43(2)	F(26)	0.4523(5)	0.1539(2)	0.5946(6)	11.7(3)
F(1)	0.3388(4)	0.0239(1)	0.0883(5)	5.7(1)	F(27)	0.4099(6)	0.0904(2)	0.5660(6)	11.1(2)
F(2)	0.5783(4)	0.0779(1)	0.1805(5)	6.6(2)	F(28)	0.2883(5)	0.1071(2)	0.3954(6)	10.0(2)
F(3)	0.3796(5)	0.0890(1)	0.1119(8)	10.8(2)	F(29)	0.1769(5)	0.1327(2)	0.9285(5)	8.2(2)
F(4)	0.4141(6)	0.0487(2)	0.2837(6)	11.1(3)	F(30)	0.3029(5)	0.1702(2)	0.7903(5)	8.6(2)
F(5)	0.5286(4)	0.0114(1)	0.1510(6)	7.8(2)	F(31)	0.1113(5)	0.1638(2)	0.7273(5)	9.2(2)
F(6)	0.4997(5)	0.0528(2)	−0.0163(5)	8.4(2)	F(32)	0.1327(6)	0.0986(2)	0.7319(7)	10.1(2)
F(7)	0.0771(4)	0.0182(2)	−0.0794(6)	9.0(2)	F(33)	0.3285(5)	0.1063(2)	0.7953(5)	7.6(2)
F(8)	0.1734(5)	0.0620(2)	0.0612(7)	10.2(2)	O(1)	0.2031(4)	0.1231(1)	0.1731(5)	4.7(2)
F(9)	0.1501(5)	0.0002(2)	0.1344(6)	10.6(2)	O(2)	0.4530(5)	0.0507(2)	0.7477(5)	5.1(2)
F(10)	0.2503(5)	−0.0220(2)	−0.0440(7)	9.9(2)	O(3)	0.4455(5)	0.2139(1)	0.7462(5)	4.9(2)
F(11)	0.2744(5)	0.0387(2)	−0.1192(6)	9.8(2)	H(1)	0.2509	0.1339	0.1302	5.7
F(12)	0.6317(4)	0.2113(1)	0.0567(5)	5.3(1)	H(2)	0.1571	0.1381	0.2011	5.7
F(13)	0.3944(4)	0.1574(1)	0.1589(5)	5.7(1)	H(3)	0.1699	0.1080	0.1287	5.7
F(14)	0.5851(5)	0.1752(2)	0.2414(6)	10.1(2)	H(4)	0.4641	0.0292	0.7271	6.2
F(15)	0.4580(5)	0.2216(1)	0.1736(6)	8.0(2)	H(5)	0.5100	0.0629	0.7327	6.2
F(16)	0.4480(4)	0.1948(2)	−0.0290(5)	7.6(2)	H(6)	0.4384	0.0516	0.8240	6.2
F(17)	0.5737(5)	0.1471(2)	0.0419(8)	10.5(2)	H(7)	0.4723	0.2040	0.6829	5.9
F(18)	0.7304(4)	0.2950(1)	−0.0790(5)	7.0(2)	H(8)	0.3807	0.2063	0.7584	5.9
F(19)	0.5850(5)	0.2751(2)	0.0728(7)	10.2(2)	H(9)	0.4441	0.2363	0.7357	5.9
F(20)	0.7761(5)	0.2555(2)	0.1099(5)	8.2(2)					
				$CsSO_3F$, **2**					
Cs(1)	0.29378(2)	0.62899(2)	0.28431(2)	2.152(3)	O(1)	0.4085(3)	0.0694(3)	0.1663(3)	2.73(5)
S(1)	0.27984(8)	0.12745(8)	0.25185(9)	1.746(10)	O(2)	0.3591(3)	0.2465(3)	0.3945(3)	3.01(5)
F(1)	0.1314(3)	0.2213(3)	0.0897(3)	4.61(6)	O(3)	0.1875(4)	−0.0043(3)	0.3070(4)	3.23(5)
				$Cs[H(SO_3F)_2]$, **3**					
Cs(1)	1/2	0.61572(3)	1/4	3.090(5)	O(2)	0.2837(3)	0.1186(4)	0.3749(4)	5.82(8)
S(1)	0.33046(6)	0.15138(9)	0.28020(9)	2.79(1)	O(3)	0.2290(2)	0.1621(3)	0.0847(3)	4.33(5)
F(1)	0.3997(3)	−0.0144(3)	0.2969(3)	6.55(6)	H(1)	1/4	1/4	0	7(1)
O(1)	0.4229(2)	0.2824(3)	0.3495(3)	4.88(5)					
				$Cs[Au(SO_3F)_4]$, **4**					
Au(1)	1/4	1/4	1/2	2.723(6)	F(2a)[c]	0.406(1)	0.543(5)	0.439(2)	9.1(8)
Cs(1)	1/2	0.3605(1)	3/4	4.49(1)	O(1)	0.2828(3)	−0.0600(7)	0.5453(3)	4.1(1)
S(1)	0.3147(1)	−0.1234(3)	0.6460(1)	4.18(4)	O(2)	0.3517(3)	0.0604(9)	0.6978(3)	5.7(1)
S(2)[b]	0.4006(6)	0.205(1)	0.4432(7)	4.7(2)	O(3)	0.3474(4)	−0.343(1)	0.6469(4)	7.0(2)
S(2a)[c]	0.412(1)	0.261(8)	0.435(2)	7.2(5)	O(4)	0.3183(3)	0.2250(8)	0.4096(3)	4.3(1)
F(1)	0.2412(3)	−0.161(1)	0.6823(4)	7.9(2)	O(5)	0.4316(3)	0.247(1)	0.5343(4)	8.3(2)
F(2)[b]	0.4083(4)	−0.062(2)	0.4374(6)	8.9(3)	O(6)	0.4409(4)	0.256(1)	0.3725(4)	9.0(2)
				$Cs_2[Pt(SO_3F)_6]$, **5**					
Pt(1)	0	0	0	1.609(8)	O(1)	0.194(1)	0.160(1)	0.1495(10)	3.2(2)
Cs(1)	1/3	−1/3	0.3331(1)	3.55(1)	O(2)	0.313(2)	−0.009(2)	0.256(2)	7.1(4)
S(1)	0.3432(5)	0.164(2)	0.2204(5)	5.5(1)	O(3)	0.432(1)	0.292(1)	0.338(1)	5.1(3)
F(1)	0.459(1)	0.218(4)	0.055(1)	10.6(4)					
				$Cs[Sb(SO_3F)_6]$, **6**					
Cs(1)	0	0	0	3.688(7)	O(1)	0.1546(2)	0.0589(2)	0.4097(2)	3.00(4)
Sb(1)	0	0	1/2	1.869(4)	O(2)	0.3558(3)	0.1830(3)	0.3234(3)	6.04(7)
S(1)	0.23450(10)	0.17073(10)	0.33273(9)	4.64(2)	O(3)	0.1648(4)	0.1553(4)	0.2342(3)	7.9(1)
F(1)	0.2413(3)	0.2824(2)	0.3919(3)	6.87(7)					

[a] $B_{eq} = (8/3)\,\pi^2\sum\sum \boldsymbol{U}_{ij}\boldsymbol{a}^*_i\boldsymbol{a}^*_j(\mathbf{a}_i\cdot\mathbf{a}_j)$. [b] Population = 0.73(1). [c] Population = 0.27.

lecular contacts for the six structures are included as Supporting Information. Structure factors are available from the authors upon request.

Results and Discussion

(a) Synthesis and Preparation of Single Crystals. The syntheses of both $Cs[Au(SO_3F)_4]$ and $Cs_2[Pt(SO_3F)_6]$ by oxidation of gold or platinum powder with bis(fluorosulfuryl peroxide), $S_2O_6F_2$, in fluorosulfuric acid, HSO_3F, in the presence of stoichiometric amounts of $CsSO_3F$ have been reported before,[6,18] together with the characterization of both salts by vibrational spectroscopy and microanalysis. It is found now that the solvent, HSO_3F, allows recrystallization of the powdery solids, formed initially, by allowing solutions to cool slowly. The only problem in the published synthetic procedures arises where $CsSO_3F$ is obtained from CsCl and HSO_3F and the byproduct HCl is not carefully removed before $S_2O_6F_2$ is added. Oxidation of HCl eventually to ClO_x derivatives, $x = 1$ or 2, causes formation of red-orange impurities, which interfere in the formation of single crystals.

Likewise the syntheses of $CsSO_3F$[16] and of $Cs[H(SO_3F)_2]$[14,17] follow published precedents. The monosolvate $Cs[H(SO_3F)_2]$ is formed exclusively when CsCl and HSO_3F are allowed to react and all volatiles are removed in vacuo with the reactor at room temperatures. A complicated apparatus as used in the synthesis of $Na[H(SO_3F)_2]$[17] is not needed. Recrystallization

Table 3. Bond Lengths (Å) with Estimated Standard Deviations in Parentheses[a]

			$[H_3O][Sb_2F_{11}]$, **1**				
Sb(1)−F(1)	2.032(4)	Sb(1)−F(2)	1.834(5)	Sb(4)−F(12)	2.016(5)	Sb(4)−F(18)	1.839(5)
Sb(1)−F(3)	1.821(6)	Sb(1)−F(4)	1.803(6)	Sb(4)−F(19)	1.799(6)	Sb(4)−F(20)	1.829(6)
Sb(1)−F(5)	1.820(5)	Sb(1)−F(6)	1.801(6)	Sb(4)−F(21)	1.842(6)	Sb(4)−F(22)	1.829(6)
Sb(2)−F(1)	2.013(5)	Sb(2)−F(7)	1.839(6)	Sb(5)−F(23)	2.023(4)	Sb(5)−F(24)	1.852(5)
Sb(2)−F(8)	1.839(6)	Sb(2)−F(9)	1.833(6)	Sb(5)−F(25)	1.824(7)	Sb(5)−F(26)	1.799(6)
Sb(2)−F(10)	1.827(6)	Sb(2)−F(11)	1.808(6)	Sb(5)−F(27)	1.802(6)	Sb(5)−F(28)	1.810(6)
Sb(3)−F(12)	2.034(4)	Sb(3)−F(13)	1.839(5)	Sb(6)−F(23)	2.028(4)	Sb(6)−F(29)	1.845(5)
Sb(3)−F(14)	1.830(6)	Sb(3)−F(15)	1.809(5)	Sb(6)−F(30)	1.846(6)	Sb(6)−F(31)	1.835(6)
Sb(3)−F(16)	1.811(5)	Sb(3)−F(17)	1.811(6)	Sb(6)−F(32)	1.785(7)	Sb(6)−F(33)	1.838(6)
			$CsSO_3F$, **2**				
Cs(1)−F(1)[a]	3.252(2)	Cs(1)−O(1)[a]	3.329(2)	Cs(1)−O(3)[f]	3.119(2)	S(1)−F(1)	1.569(2)
Cs(1)−O(1)[b]	3.220(2)	Cs(1)−O(2)	3.223(3)	S(1)−O(1)	1.458(2)	S(1)−O(2)	1.437(2)
Cs(1)−O(2)[c]	3.265(2)	Cs(1)−O(2)[d]	3.115(2)	S(1)−O(3)	1.436(2)		
Cs(1)−O(3)[e]	3.151(2)	Cs(1)−O(3)[c]	3.316(3)				
			$Cs[H(SO_3F)_2]$, **3**				
Cs(1)−F(1)[a]	3.303(2)	Cs(1)−O(1)	3.131(2)	S(1)−F(1)	1.531(2)	S(1)−O(1)	1.406(2)
Cs(1)−O(1)[b]	3.354(3)	Cs(1)−O(2)[c]	3.196(3)	S(1)−O(2)	1.399(3)	S(1)−O(3)	1.471(2)
Cs(1)−O(2)[b]	3.530(3)	Cs(1)−O(3)[d]	3.464(2)	O(3)−H(1)	1.210(2)		
			$Cs[Au(SO_3F)_4]$, **4**				
Au(1)−O(1)	1.968(4)	Au(1)−O(4)	1.976(4)	S(1)−O(3)	1.402(6)	S(2)−F(2)	1.56(1)
Cs(1)−F(2a)[a]	3.56(3)	Cs(1)−O(2)	3.115(5)	S(2)−O(4)	1.44(1)	S(2)−O(5)	1.35(1)
Cs(1)−O(3)[b]	3.295(6)	Cs(1)−O(5)	3.202(5)	S(2)−O(6)	1.41(1)	S(2a)−F(2a)	1.65(4)
Cs(1)−O(6)[a]	3.177(7)	S(1)−F(1)	1.523(6)	S(2a)−O(4)	1.64(2)	S(2a)−O(5)	1.42(3)
S(1)−O(1)	1.508(4)	S(1)−O(2)	1.393(5)	S(2a)−O(6)	1.14(3)		
			$Cs_2[Pt(SO_3)_2]$, **5**				
Pt(1)−O(1)	1.987(8)	Cs(1)−F(1)[a]	3.371(9)	S(1)−F(1)	1.555(9)	S(1)−O(1)	1.44(1)
Cs(1)−O(2)	3.10(1)	Cs(1)−O(3)[b]	3.184(9)	S(1)−O(2)	1.48(2)	S(1)−O(3)	1.36(1)
			$Cs[Sb(SO_3F)_6]$, **6**				
Cs(1)−O(2)[a]	3.241(3)	Cs(1)−O(3)	3.413(4)	S(1)−O(1)	1.516(2)	S(1)−O(2)	1.396(3)
Sb(1)−O(1)	1.955(2)	S(1)−F(1)	1.486(3)	S(1)−O(3)	1.409(4)		

[a] Superscripts refer to symmetry operations: for **2**, (a) $^1/_2 - x$, $^1/_2 + y$, $-z$, (b) $-^1/_2 + x$, $^1/_2 - y$, z, (c) $^1/_2 - x$, $^1/_2 + y$, $1 - z$, (d) $1 - x$, $1 - y$, $1 - z$, (e) $^1/_2 + x$, $^1/_2 - y$, z, (f) x, $1 + y$, z; for **3**, (a) x, $1 + y$, z, (b) $1 - x$, $1 - y$, $1 - z$, (c) $^1/_2 + x$, $^1/_2 + y$, z, (d) $^1/_2 - x$, $^1/_2 - y$, $-z$; for **4**, (a) x, $1 - y$, $^1/_2 + z$, (b) x, $1 + y$, z; for **5**, (a) $x - y$, $-y$, $-z$, (b) y, $-1 + x$, $1 - z$; for **6**, (a) $^2/_3 - x$, $^1/_3 - y$, $^1/_3 - z$.

from HSO_3F produces single crystals, which are separated by filtration inside the drybox.

Conversion of $Cs[H(SO_3F)_2]$ to $CsSO_3F$ requires prolonged heating (3 days) at 120 °C *in vacuo* until all HSO_3F is removed. Single crystals are obtained by recrystallization of crude $CsSO_3F$ from deionized water as described previously.[31] Trace amounts of acid will cause rapid solvolysis of the sulfur−fluorine moiety and will yield Cs_2SO_4 or $Cs[HSO_4]$ instead.

The formation of $[H_3O][Sb_2F_{11}]$ from magic acid, HSO_3F-SbF_5, with a SbF_5 concentration of 30 mol % or higher is surprising and highly unexpected for two reasons: (a) the formation of the oxonium ion $[H_3O]^+$, without the deliberate addition of H_2O as reported previously,[25a] and (b) the presence of $[Sb_2F_{11}]^-$ as counteranion,[23b,24,25] which is found in magic acid in very low concentrations only.

As seen in Figure 1 a plot of ^1H chemical shifts of magic acid against the SbF_5 concentration, a single line resonance between ∼9.5 and ∼8 ppm is attributed to $[H_3O]^+$, while a second single line resonance between 9.5 and 11.2 ppm appears to be caused by the "acidic" proton of the two conjugate pairs $HSO_3F-H_2SO_3F^+$ and $HF-H_2F^+$.[23b] While the protonation of H_2O in magic acid is expected on account of the excellent proton acceptor ability of H_2O in strong protonic acids, the presence of water is surprising. A possible source is the dehydration of fluorosulfuric acid according to

$$2HSO_3F \rightleftarrows H_2O + S_2O_5F_2 \qquad (3)$$

However this is not a facile process at room temperature[47] and requires the presence of a dehydrating agent like e.g. As_4O_{10}.[48] More convincingly there is no evidence for the anhydride $S_2O_5F_2$ in the ^{19}F-NMR spectrum of magic acid at any SbF_5 concentration. The chemical shift of $S_2O_5F_2$ at 49 ppm[49] is well separated from other ^{19}F resonances at 45−38 ppm[23−25] in the system to allow its detection. Its consumption via a chemical reaction is improbable as well, because the reaction of SbF_5 with SO_3, presumably via some fluoride−fluorosulfonates of antimony(V) is a viable synthetic route to $S_2O_5F_2$.[47]

The second alternative explanation for the formation of $[H_3O]^+$ is the interaction of HF with glass. This assumption is supported by the observation of SiF_4 (or $[SiF_6]^{2-}$) in the ^{19}F NMR spectra of magic acid in substantial quantities and visible signs of etching of glassware after prolonged standing. A recent redetermination of the acidity of anhydrous hydrogen fluoride[50] has concluded that both HF and HSO_3F have identical $-H_o$ values of 15.1. This in turn makes it unlikely that HF will be extensively protonated by fluorosulfuric acid to H_2F^+. This seemed probable, based on older $-H_o$ values of ∼11.0 for HF,[2] and it was hence assumed that HF will not attack glass, when dissolved in HSO_3F where it is extensively protonated to H_2F^+.

Small amounts of HF impurities, present either in SbF_5 or in HSO_3F may account for some of the $[H_3O]^+$. More important in our opinion appears to be the solvolysis of antimony(V) fluoride in HSO_3F according to the general net reaction

$$SbF_5 + nHSO_3F \rightarrow SbF_{5-n}(SO_3F)_n + nHF \quad n = 1, 2, \text{ or } 3 \qquad (4)$$

which is consistent with the observed product distribution in

(47) Hayek, E.; Koller, W. *Monatsh. Chem.* **1951**, *82*, 942.

(48) Hayek, E.; Aignesberger, A.; Engelbrecht, A. *Monatsh. Chem.* **1955**, *86*, 735.

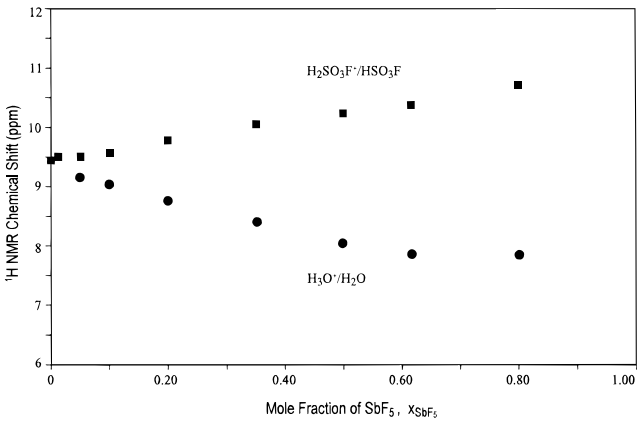

Figure 1. Dependence of ^1H NMR chemical shifts on SbF_5 concentration in the HSO_3F/SbF_5 system.

magic acid, as studied by ^{19}F-NMR.[23b,25] Both $[SbF_6]^-$ and, at higher SbF_5 concentrations $[Sb_2F_{11}]^-$, are only minor constituents among a number of complex anions with fluoro and fluorosulfato substituents. This is not consistent with the suggested ligand redistribution[23a] of the anion $[SbF_5(SO_3F)]^-$—formed initially at low SbF_5 concentrations—by the direct combination

$$SbF_5 + SO_3F^- \rightarrow [SbF_5(SO_3F)]^- \quad (5)$$

and subsequent ligand redistribution via F^- vs SO_3F^- interchange according to

$$2[SbF_5(SO_3F)]^- \rightleftarrows [SbF_6]^- + [SbF_4(SO_3F)_2]^- \quad (6)$$

should result in equimolar concentrations of the two products, $[SbF_6]^-$ and the two isomers, *cis*- and *trans*-$[SbF_4(SO_3F)_2]^-$. In reality $[SbF_4(SO_3F)_2]^-$ is present in a 10−30-fold excess depending on the SbF_5 concentration, which is consistent with extensive solvolysis of SbF_5 in HSO_3F, in addition to ligand redistribution.

The exclusive formation of solid, crystalline $[H_3O][Sb_2F_{11}]$ from magic acid with SbF_5 present in concentrations of 30 mol % or higher is due to the limited solubility of this salt in magic acid. The polymeric structure of $[H_3O][Sb_2F_{11}]$ (vide infra) produced by extensive interionic hydrogen bonding is seen as a reason for the low solubility. Slow formation of $[H_3O][Sb_2F_{11}]$ over several weeks eventually produces large amounts of single crystals, which do not require any further recrystallization. The $[Sb_2F_{11}]^-$ anion, which as stated is only a minor constituent in magic acid at high SbF_5 concentrations, must re-form slowly via ligand exchange equilibria.[23a]

While the formation of $[H_3O][Sb_2F_{11}]$ from magic acid is accidental, the related oxonium fluoroantimonate, $[H_3O][SbF_6]$, is formed in a stoichiometric reaction in HF[26] according to

$$HF\ (DF) + H_2O\ (D_2O) + SbF_5 \xrightarrow{HF\ (DF)} [H_3O][SbF_6]\ ([D_3O][SbF_6]) \quad (7)$$

and is soluble in HF or DF and according to our observations[23b] also in magic acid. The salt has a cubic, less complicated structure[27] than $[H_3O][Sb_2F_{11}]$.

There are many precedents for the formation of $Cs[Sb(SO_3F)_6]$ in a simple, one-step reaction according to

$$2CsSO_3F + 2Sb + 5S_2O_6F_2 \xrightarrow[HSO_3F]{25\ °C,\ 12\ h} 2Cs[Sb(SO_3F)_6] \quad (8)$$

Among them, the analogous synthesis of $Cs_2[Sn(SO_3F)_6]$ is noteworthy,[20] because the salt has an anion isoelectronic to $[Sb(SO_3F)_6]^-$. There are also precedents of the type $Cs[M(SO_3F)_6]$, M = Nb or Ta,[51] but in all these cases characterization of the salts is accomplished by spectroscopic means only. All Cs^+ salts with hexakis(fluorosulfato)metalate anions show fairly high thermal stabilities, and $Cs[Sb(SO_3F)_6]$ is no exception and decomposes at 149 °C. The synthesis is straightforward as suggested by eq 8, but we have noticed the formation of a very finely distributed white precipitate during the oxidation of antimony, which is formed in such small amounts that a complete identification has not been possible. This white solid remains insoluble in HSO_3F even at elevated temperatures. This is not the case for polymeric $[Sb(SO_3F)_3]_x$, a possible intermediate in the oxidation of Sb by $S_2O_6F_2$, which can be recrystallized from fluorosulfuric acid and whose molecular structure we have reported previously.[15] It is hence necessary to recrystallize $Cs[Sb(SO_3F)_6]$ from HSO_3F to obtain suitable samples for a molecular structure determination and a vibrational analysis.

The facile formation of $Cs[Sb(SO_3F)_6]$ as described here suggests that the homoleptic conjugate superacid system $HSO_3F-Sb(SO_3F)$ which undergoes proton transfer according to

$$2HSO_3F + Sb(SO_3F)_5(solv) \rightleftarrows H_2SO_3F^+ + [Sb(SO_3F)_6]^-(solv) \quad (9)$$

should exist and should exhibit high concentration dependent acidities. We are currently attempting to synthesize the Lewis acid $Sb(SO_3F)_5$ either as a pure compound or in HSO_3F solution, by the oxidation of antimony with bis(fluorosulfuryl) peroxide in HSO_3F, in analogy to the in situ formation of $M(SO_3F)_5(solv)$,[51] M = Nb or Ta.

(b) The Molecular Structures of Superacid Anions. A. Description of the Molecular Structures and Comparison to Related Structures. The molecular structures reported here are conveniently arranged in three groups and discussed in this order: (i) $[H_3O][Sb_2F_{11}]$, (**1**), oxonium undecafluorodiantimonate(V), which is as discussed above obtained from magic acid; (ii) $CsSO_3F$, (**2**) cesium fluorosulfate and its monosolvate $Cs[H(SO_3F)_2]$, (**3**), which are obtained from the Brönsted superacid HSO_3F; (iii) the conjugate superacid anions $Cs[Au(SO_3F)_4]$, (**4**), cesium tetrakis(fluorosulfato)aurate(III), $Cs_2[Pt(SO_3F)_6]$, (**5**), cesium hexakis(fluorosulfato)platinate(IV), derived from the corresponding known noble metal superacid systems,[6,18] and $Cs[Sb(SO_3F)_6]$, (**6**), cesium hexakis(fluorosulfato)antimonate(V), where the corresponding conjugate superacid system remains to be fully explored.

(i) $[H_3O][Sb_2F_{11}]$. Among the six structures reported in this study, this salt is unique on account of the presence of the molecular cation $[H_3O]^+$. Since there are in addition to $[H_3O][SbF_6]$, which has been mentioned already,[26,27] other structure determinations of oxonium salts with fluorometalate anions like $[H_3O][TiF_5]$[52] and $[H_3O][BF_4]$[53] reported, the emphasis in our discussion, consistent with the intent of this study, will be largely on the $[Sb_2F_{11}]^-$ anion and on the effect hydrogen bonding has on this species.

Even though the rather asymmetric O−H--F bond distances and O--F nonbonded contacts are slightly longer (average value 2.759 Å) and cover a wider range (2.553(8)−2.903(9) Å)

(49) (a) Gillespie, R. J.; Robinson, E. A. *Can. J. Chem.* **1962**, *40*, 675. (b) Lustig, M. *Inorg. Chem.* **1965**, *4*, 1828.
(50) Gillespie, R. J.; Liang, J. *J. Am. Chem. Soc.* **1988**, *110*, 6053.
(51) Cicha, W. V.; Aubke, F. *J. Am. Chem. Soc.* **1989**, *111*, 4328.
(52) Cohen, S.; Selig, H.; Gut, R. *J. Fluorine Chem.* **1982**, *20*, 349.
(53) Mootz, D.; Steffen, M. *Z. Anorg. Allg. Chem.* **1981**, *42*, 193.

Table 4. Bond Angles (deg) with Estimated Standard Deviations in Parentheses[a]

$[H_3O][Sb_2F_{11}]$, **1**

F(1)−Sb(1)−F(2)	179.5(2)	F(1)−Sb(1)−F(3)	85.9(2)	F(12)−Sb(4)−F(21)	85.8(2)	F(12)−Sb(4)−F(22)	84.4(2)
F(1)−Sb(1)−F(4)	85.8(3)	F(1)−Sb(1)−F(5)	83.5(2)	F(18)−Sb(4)−F(19)	93.8(3)	F(18)−Sb(4)−F(20)	95.8(3)
F(1)−Sb(1)−F(6)	86.4(3)	F(2)−Sb(1)−F(3)	94.6(3)	F(18)−Sb(4)−F(21)	95.2(3)	F(18)−Sb(4)−F(22)	94.7(3)
F(2)−Sb(1)−F(4)	94.1(3)	F(2)−Sb(1)−F(5)	96.0(3)	F(19)−Sb(4)−F(20)	91.1(4)	F(19)−Sb(4)−F(21)	171.0(3)
F(2)−Sb(1)−F(6)	93.6(3)	F(3)−Sb(1)−F(4)	89.9(4)	F(19)−Sb(4)−F(22)	90.0(4)	F(20)−Sb(4)−F(21)	88.7(3)
F(3)−Sb(1)−F(5)	169.4(3)	F(3)−Sb(1)−F(6)	89.6(4)	F(20)−Sb(4)−F(22)	169.4(3)	F(21)−Sb(4)−F(22)	88.6(3)
F(4)−Sb(1)−F(5)	90.1(4)	F(4)−Sb(1)−F(6)	172.2(3)	F(23)−Sb(5)−F(24)	178.4(2)	F(23)−Sb(5)−F(25)	86.0(3)
F(5)−Sb(1)−F(6)	88.9(3)	F(1)−Sb(2)−F(7)	177.3(3)	F(23)−Sb(5)−F(26)	84.2(2)	F(23)−Sb(5)−F(27)	86.6(2)
F(1)−Sb(2)−F(8)	85.0(2)	F(1)−Sb(2)−F(9)	86.2(2)	F(23)−Sb(5)−F(28)	86.2(2)	F(24)−Sb(5)−F(25)	95.4(3)
F(1)−Sb(2)−F(10)	85.5(2)	F(1)−Sb(2)−F(11)	84.4(3)	F(24)−Sb(5)−F(26)	95.1(3)	F(24)−Sb(5)−F(27)	92.0(3)
F(7)−Sb(2)−F(8)	92.5(3)	F(7)−Sb(2)−F(9)	94.9(3)	F(24)−Sb(5)−F(28)	94.5(3)	F(25)−Sb(5)−F(26)	89.1(4)
F(7)−Sb(2)−F(10)	97.0(3)	F(7)−Sb(2)−F(11)	94.6(3)	F(25)−Sb(5)−F(27)	172.5(3)	F(25)−Sb(5)−F(28)	87.4(4)
F(8)−Sb(2)−F(9)	89.7(4)	F(8)−Sb(2)−F(10)	170.4(3)	F(26)−Sb(5)−F(27)	91.4(4)	F(26)−Sb(5)−F(28)	170.0(3)
F(8)−Sb(2)−F(11)	90.8(4)	F(9)−Sb(2)−F(10)	88.6(4)	F(27)−Sb(5)−F(28)	90.9(4)	F(23)−Sb(6)−F(29)	177.9(2)
F(9)−Sb(2)−F(11)	170.5(3)	F(10)−Sb(2)−F(11)	89.3(4)	F(23)−Sb(6)−F(30)	84.9(2)	F(23)−Sb(6)−F(31)	85.6(2)
F(12)−Sb(3)−F(13)	179.1(2)	F(12)−Sb(3)−F(14)	84.8(2)	F(23)−Sb(6)−F(32)	86.5(3)	F(23)−Sb(6)−F(33)	85.5(2)
F(12)−Sb(3)−F(15)	85.6(2)	F(12)−Sb(3)−F(16)	85.7(2)	F(29)−Sb(6)−F(30)	93.7(3)	F(29)−Sb(6)−F(31)	95.9(3)
F(12)−Sb(3)−F(17)	86.4(2)	F(13)−Sb(3)−F(14)	94.7(3)	F(29)−Sb(6)−F(32)	95.0(3)	F(29)−Sb(6)−F(33)	92.9(3)
F(13)−Sb(3)−F(15)	93.6(2)	F(13)−Sb(3)−F(16)	94.8(2)	F(30)−Sb(6)−F(31)	88.0(3)	F(30)−Sb(6)−F(32)	171.4(3)
F(13)−Sb(3)−F(17)	94.3(3)	F(14)−Sb(3)−F(15)	89.6(3)	F(30)−Sb(6)−F(33)	87.1(3)	F(31)−Sb(6)−F(32)	91.0(4)
F(14)−Sb(3)−F(16)	170.4(3)	F(14)−Sb(3)−F(17)	88.2(4)	F(31)−Sb(6)−F(33)	170.2(3)	F(32)−Sb(6)−F(33)	92.5(3)
F(15)−Sb(3)−F(16)	89.3(3)	F(15)−Sb(3)−F(17)	171.9(3)	Sb(1)−F(1)−Sb(2)	149.4(3)	Sb(3)−F(12)−Sb(4)	148.3(3)
F(16)−Sb(3)−F(17)	91.6(4)	F(12)−Sb(4)−F(18)	178.6(2)	Sb(5)−F(23)−Sb(6)	145.9(2)		

$CsSO_3F$, **2**

F(1)[a]−Cs(1)−O(1)[a]	41.97(5)	F(1)[a]−Cs(1)−O(1)[b]	107.53(6)	O(2)[d]−Cs(1)−O(3)[e]	61.42(7)	O(2)[d]−Cs(1)−O(3)[c]	66.75(6)
F(1)[a]−Cs(1)−O(2)	113.64(6)	F(1)[a]−Cs(1)−O(2)[c]	147.75(6)	O(2)[d]−Cs(1)−O(3)[f]	79.14(7)	O(3)[e]−Cs(1)−O(3)[c]	97.40(6)
F(1)[a]−Cs(1)−O(2)[d]	105.48(6)	F(1)[a]−Cs(1)−O(3)[e]	69.47(7)	O(3)[e]−Cs(1)−O(3)[f]	125.00(7)	O(3)[c]−Cs(1)−O(3)[f]	100.48(5)
F(1)[a]−Cs(1)−O(3)[c]	166.87(6)	F(1)[a]−Cs(1)−O(3)[f]	87.91(7)	F(1)−S(1)−O(1)	102.3(1)	F(1)−S(1)−O(2)	106.3(1)
O(1)[a]−Cs(1)−O(1)[b]	65.57(6)	O(1)[a]−Cs(1)−O(2)	96.32(6)	F(1)−S(1)−O(3)	107.8(2)	O(1)−S(1)−O(2)	113.6(1)
O(1)[a]−Cs(1)−O(2)[c]	133.43(6)	O(1)[a]−Cs(1)−O(2)[d]	147.21(6)	O(1)−S(1)−O(3)	112.7(1)	O(2)−S(1)−O(3)	113.2(1)
O(1)[a]−Cs(1)−O(3)[e]	95.40(6)	O(1)[a]−Cs(1)−O(3)[c]	143.82(6)	Cs(1)[g]−F(1)−S(1)	107.2(1)	Cs(1)[e]−O(1)−Cs(1)[g]	114.43(6)
O(1)[a]−Cs(1)−O(3)[f]	99.49(7)	O(1)[b]−Cs(1)−O(2)	68.41(6)	Cs(1)[e]−O(1)−S(1)	138.0(1)	Cs(1)[g]−O(1)−S(1)	107.1(1)
O(1)[b]−Cs(1)−O(2)[c]	79.42(6)	O(1)[b]−Cs(1)−O(2)[d]	146.83(6)	Cs(1)−O(2)−Cs(1)[h]	114.98(7)	Cs(1)−O(2)−Cs(1)[d]	84.69(6)
O(1)[b]−Cs(1)−O(3)[e]	129.04(6)	O(1)[b]−Cs(1)−O(3)[c]	80.20(6)	Cs(1)−O(2) −S(1)	117.6(1)	Cs(1)[h]−O(2)−Cs(1)[d]	85.61(6)
O(1)[b]−Cs(1)−O(3)[f]	105.17(6)	O(2)−Cs(1)−O(2)[c]	98.31(5)	Cs(1)[h]−O(2) −S(1)	102.9(1)	Cs(1)[d]−O(2)−S(1)	148.0(1)
O(2)−Cs(1)−O(2)[d]	95.31(6)	O(2)−Cs(1)−O(3)[e]	67.49(6)	Cs(1)[b]−O(3) −Cs(1)[i]	87.50(6)	Cs(1)[b]−O(3)−Cs(1)[h]	82.60(6)
O(2)−Cs(1)−O(3)[c]	58.58(6)	O(2)−Cs(1)−O(3)[f]	158.42(6)	Cs(1)[b]−O(3) −S(1)	142.7(1)	Cs(1)[i]−O(3) −Cs(1)[h]	116.45(8)
O(2)[c]−Cs(1)−O(2)[d]	74.49(5)	O(2)[c]−Cs(1)−O(3)[e]	131.01(7)	Cs(1)[i]−O(3) −S(1)	122.0(1)	Cs(1)[h]−O(3) −S(1)	100.7(1)
O(2)[c]−Cs(1)−O(3)[c]	42.74(6)	O(2)[c]−Cs(1)−O(3)[f]	60.12(6)				

$Cs[H(SO_3F)_2]$, **3**

F(1)[a]−Cs(1)−F(1)[e]	60.1(1)	F(1)[a]−Cs(1)−O(1)	115.76(8)	O(2)[c]−Cs(1)−O(2)[f]	114.25(6)	O(2)[c]−Cs(1)−O(2)[b]	65.24(8)
F(1)[a]−Cs(1)−O(1)[f]	94.83(6)	F(1)[a]−Cs(1)−O(1)[g]	171.97(6)	O(2)[c]−Cs(1)−O(3)[d]	120.99(8)	O(2)[c]−Cs(1)−O(3)[i]	59.59(6)
F(1)[a]−Cs(1)−O(1)[b]	60.61(6)	F(1)[a]−Cs(1)−O(2)[c]	115.57(8)	O(2)[f]−Cs(1)−O(2)[b]	108.85(9)	O(2)[f]−Cs(1)−O(3)[d]	74.46(7)
F(1)[a]−Cs(1)−O(2)[h]	63.66(7)	F(1)[a]−Cs(1)−O(2)[f]	59.01(6)	O(2)[f]−Cs(1)−O(3)[i]	171.61(6)	O(3)[d]−Cs(1)−O(3)[i]	103.37(8)
F(1)[a]−Cs(1)−O(2)[b]	60.51(6)	F(1)[a]−Cs(1)−O(3)[d]	117.27(6)	F(1)−S(1)−O(1)	104.8(2)	F(1)−S(1)−O(2)	105.3(2)
F(1)[a]−Cs(1)−O(3)[i]	127.96(6)	O(1)−Cs(1)−O(1)[f]	127.40(6)	F(1)−S(1)−O(3)	101.7(1)	O(1)−S(1)−O(2)	116.3(2)
O(1)−Cs(1)−O(1)[g]	69.2(1)	O(1)−Cs(1)−O(1)[b]	77.24(7)	O(1)−S(1)−O(3)	113.8(1)	O(2)−S(1)−O(3)	113.0(2)
O(1)−Cs(1)−O(2)[c]	115.55(7)	O(1)−Cs(1)−O(2)[h]	65.18(8)	Cs(1)[j]−F(1)−S(1)	168.8(1)	Cs(1)−O(1)−Cs(1)[b]	102.76(7)
O(1)−Cs(1)−O(2)[f]	124.44(6)	O(1)−Cs(1)−O(2)[b]	113.08(6)	Cs(1)−O(1)−S(1)	144.1(1)	Cs(1)[b]−O(1)−S(1)	105.2(1)
O(1)−Cs(1)−O(3)[d]	59.78(5)	O(1)−Cs(1)−O(3)[i]	58.86(7)	Cs(1)[k]−O(2)−Cs(1)[b]	114.76(8)	Cs(1)[k]−O(2)−S(1)	131.6(2)
O(1)[f]−Cs(1)−O(1)[b]	152.84(8)	O(1)[f]−Cs(1)−O(2)[c]	82.98(7)	Cs(1)[b]−O(2)−S(1)	97.4(1)	Cs(1)[d]−O(3)−S(1)	136.0(1)
O(1)[f]−Cs(1)−O(2)[h]	96.83(7)	O(1)[f]−Cs(1)−O(2)[f]	40.41(6)	Cs(1)[d]−O(3)−H(1)	100.2(1)	S(1)−O(3)−H(1)	117.1(2)
O(1)[f]−Cs(1)−O(2)[b]	119.23(6)	O(1)[f]−Cs(1)−O(3)[d]	68.43(6)	O(3)−H(1)−O(3)[d]	180.0		
O(1)[f]−Cs(1)−O(3)[i]	131.20(6)	O(2)[c]−Cs(1)−O(2)[h]	179.2(1)				

$Cs[Au(SO_3F)_4]$, **4**

O(1)−Au(1)−O(1)[c]	180.0	O(1)−Au(1)−O(4)	88.8(2)	F(1)−S(1)−O(2)	105.1(4)	F(1)−S(1)−O(3)	104.3(4)
O(1)−Au(1)−O(4)[c]	91.2(2)	O(4)−Au(1)−O(4)[c]	180.0	O(1)−S(1)−O(2)	112.4(3)	O(1)−S(1)−O(3)	107.5(3)
F(2a)[a]−Cs(1)−F(2a)[d]	161.9(9)	F(2a)[a]−Cs(1)−O(2)	76.6(4)	O(2)−S(1)−O(3)	123.3(3)	F(2)−S(2)−O(4)	99.0(6)
F(2a)[a]−Cs(1)−O(2)[e]	114.1(4)	F(2a)[a]−Cs(1)−O(3)[b]	78.4(4)	F(2)−S(2)−O(5)[+]	102.2(7)	F(2)−S(2)−O(6)	96.1(6)
F(2a)[a]−Cs(1)−O(3)[f]	92.1(4)	F(2a)[a]−Cs(1)−O(5)	130.9(4)	O(4)−S(2)−O(5)	119.5(7)	O(4)−S(2)−O(6)	111.4(8)
F(2a)[a]−Cs(1)−O(5)[e]	53.9(4)	F(2a)[a]−Cs(1)−O(6)[a]	35.7(5)	O(5)−S(2)−O(6)	121.5(8)	F(2a)−S(2a)−O(4)	93(2)
F(2a)[a]−Cs(1)−O(6)[d]	126.2(5)	O(2)−Cs(1)−O(2)[e]	111.8(2)	F(2a)−S(2a)−O(5)	91(2)	F(2a)−S(2a)−O(6)	95(2)
O(2)−Cs(1)−O(3)[b]	67.2(2)	O(2)−Cs(1)−O(3)[f]	167.3(1)	O(4)−S(2a)−O(5)	103(1)	O(4)−S(2a)−O(6)	114(2)
O(2)−Cs(1)−O(5)	61.1(1)	O(2)−Cs(1)−O(5)[e]	104.5(1)	O(5)−S(2a)−O(6)	140(2)	Cs(1)−F(2a)−S(2)	102.2(10)
O(2)−Cs(1)−O(6)[a]	99.9(2)	O(2)−Cs(1)−O(6)[d]	128.2(1)	Cs(1)−F(2a)−S(2a)	94(1)	Au(1)−O(1)−S(1)	125.2(3)
O(3)[b]−Cs(1)−O(3)[f]	116.8(2)	O(3)[b]−Cs(1)−O(5)	63.4(2)	Cs(1)−O(2)−S(1)	147.2(4)	Cs(1)[g]−O(3)−S(1)	141.2(3)
O(3)[b]−Cs(1)−O(5)[e]	131.6(2)	O(3)[b]−Cs(1)−O(6)[a]	63.5(2)	Au(1)−O(4)−S(2)	119.8(4)	Au(1)−O(4)−S(2a)	124(1)
O(3)[b]−Cs(1)−O(6)[d]	73.1(2)	O(5)−Cs(1)−O(5)[e]	156.1(3)	Cs(1)−O(5)−S(2)	177.9(6)	Cs(1)−O(5)−S(2a)	162(1)
O(5)−Cs(1)−O(6)[a]	126.8(2)	O(5)−Cs(1)−O(6)[d]	72.0(2)	Cs(1)[d]−O(6)−S(2)	147.3(5)	Cs(1)[d]−O(6)−S(2a)	133(2)
O(6)[a]−Cs(1)−O(6)[d]	90.6(3)	F(1)−S(1)−O(1)	101.7(3)				

$Cs[Pt(SO_3F)_6]$, **5**

O(1)−Pt(1)−O(1)[c]	90.5(4)	O(1)−Pt(1)−O(1)[e]	72.0(5)	O(2)−Cs(1)−O(3)[k]	88.0(3)	O(3)[b]−Cs(1)−O(3)[j]	64.9(3)
O(1)−Pt(1)−O(1)[f]	146.5(5)	O(1)−Pt(1)−O(1)[a]	117.3(5)	F(1)−S(1)−O(1)	100.6(9)	F(1)−S(1)−O(2)	102(1)

Table 4 (Continued)

F(1)[a]−Cs(1)−F(1)[g]	49.7(3)	F(1)[a]−Cs(1)−O(2)	52.9(5)	F(1)−S(1)−O(3)	104.5(10)	O(1)−S(1)−O(2)	111.6(8)
F(1)[a]−Cs(1)−O(2)[h]	83.8(6)	F(1)[a]−Cs(1)−O(2)[i]	102.5(5)	O(1)−S(1)−O(3)	114(1)	O(2)−S(1)−O(3)	120(1)
F(1)[a]−Cs(1)−O(3)[b]	158.5(6)	F(1)[a]−Cs(1)−O(3)[j]	114.4(3)	Cs(1)[l]−F(1)−S(1)	172(1)	Pt(1)−O(1)−S(1)	135.3(7)
F(1)[a]−Cs(1)−O(3)[k]	135.7(5)	O(2)−Cs(1)−O(2)[h]	116.5(2)	Cs(1)−O(2)−S(1)	167.7(8)	Cs(1)[m]−O(3)−S(1)	133.6(9)
O(2)−Cs(1)−O(3)[b]	137.9(4)	O(2)−Cs(1)−O(3)[j]	74.8(4)				
			$Cs[Sb(SO_3F)_6]$, **6**				
O(2)[a]−Cs(1)−O(2)[b]	180.0	O(2)[a]−Cs(1)−O(2)[c]	119.865(7)	O(1)−Sb(1)−O(1)[e]	92.15(9)	O(1)−Sb(1)−O(1)[j]	180.0
O(2)[a]−Cs(1)−O(2)[d]	60.135(8)	O(2)[a]−Cs(1)−O(3)	58.11(9)	O(1)−Sb(1)−O(1)[k]	87.85(9)	F(1)−S(1)−O(1)	103.5(1)
O(2)[a]−Cs(1)−O(3)[e]	116.68(7)	O(2)[a]−Cs(1)−O(3)[f]	89.31(10)	F(1)−S(1)−O(2)	111.1(2)	F(1)−S(1)−O(3)	106.4(2)
O(2)[a]−Cs(1)−O(3)[g]	121.89(9)	O(2)[a]−Cs(1)−O(3)[h]	63.32(7)	O(1)−S(1)−O(2)	108.0(2)	O(1)−S(1)−O(3)	109.0(2)
O(2)[a]−Cs(1)−O(3)[i]	90.69(10)	O(3)−Cs(1)−O(3)[e]	58.59(9)	O(2)−S(1)−O(3)	117.9(2)	Sb(1)−O(1)−S(1)	136.6(1)
O(3)−Cs(1)−O(3)[g]	180.0	O(3)−Cs(1)−O(3)[h]	121.41(9)	Cs(1)[l]−O(2)−S(1)	155.5(2)	Cs(1)−O(3)−S(1)	155.6(2)

[a] Superscripts refer to the symmetry operations: for **2**; (a) $^1/_2 - x, ^1/_2 + y, -z$, (b) $-^1/_2 + x, ^1/_2 - y, z$, (c) $^1/_2 - x, ^1/_2 + y, 1 - z$, (d) $1 - x, 1 - y, 1 - z$, (e) $^1/_2 + x, ^1/_2 - y, z$, (f) $x, 1 + y, z$, (g) $^1/_2 - x, -^1/_2 + y, -z$, (h) $^1/_2 - x, -^1/_2 + y, 1 - z$, (i) $x, -1 + y, z$; for **3**, (a) $x, 1 + y, z$, (b) $1 - x, 1 - y, 1 - z$, (c) $^1/_2 + x, ^1/_2 + y, z$, (d) $^1/_2 - x, ^1/_2 - y, -z$, (e) $1 - x, 1 + y, ^1/_2 - z$, (f) $x, 1 - y, -^1/_2 + z$, (g) $1 - x, y, ^1/_2 - z$, (h) $^1/_2 - x, ^1/_2 + y, ^1/_2 - z$, (i) $^1/_2 + x, ^1/_2 - y, ^1/_2 + z$, (j) $x, -1 + y, z$, (k) $-^1/_2 + x, -^1/_2 + y, z$; for **4**, (a) $x, 1 - y, ^1/_2 + z$, (b) $x, 1 + y, z$, (c) $^1/_2 - x, ^1/_2 - y, 1 - z$, (d) $1 - x, 1 - y, 1 - z$, (e) $1 - x, y, ^3/_2 - z$, (f) $1 - x, 1 + y, ^3/_2 - z$, (g) $x, -1 + y, z$; for **5**, (a) $x - y, -y, -z$, (b) $y, -1 + x, 1 - z$, (c) $-y, x - y, z$, (d) $-x + y, -x, z$, (e) $y, x, -z$, (f) $-x, -x + y, -z$, (g) $y, -1 + x, -z$, (h) $-y, -1 + x - y, z$, (i) $1 - x + y, -x, z$, (j) $x - y, -z, 1 - z$, (k) $1 - x, -x + y, 1 - z$, (l) $1 + y, x, z$, (m) $1 + y, x, 1 + z$; for **6**, (a) $^2/_3 - x, ^1/_3 - y, ^1/_3 - z$, (b) $-^2/_3 + x, -^1/_3 + y - ^1/_3 + z$, (c) $-^1/_3 + x - y, -^2/_3 + x, ^1/_3 - z$, (d) $^1/_3 - y, -^1/_3 + x - y, -^1/_3 + z$, (e) $-y, x - y, z$, (f) $-x + y, -x, z$, (g) $-x, -y, -z$, (h) $y, -x + y, -z$, (i) $x - y, x, -z$, (j) $-x, -y, 1 - z$, (k) $y, -x + y, 1 - z$, (l) $^2/_3 + x, ^1/_3 + y, ^1/_3 + z$.

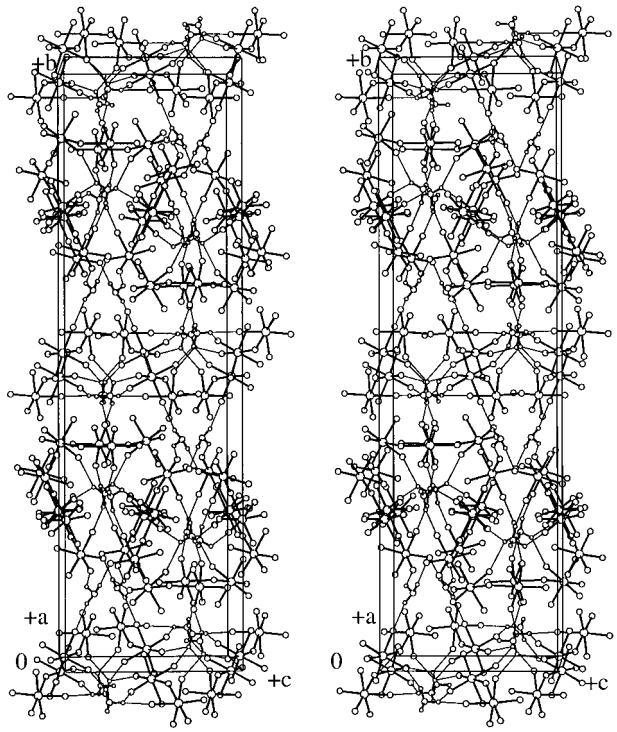

Figure 2. Stereoscopic view along *a* of the unit cell of $[H_3O][Sb_2F_{11}]$.

compared to 2.622(12)−2.713(10) Å for $[H_3O][SbF_6]$,[27] 2.522(6)−2.558(5) Å for $[H_3O][TiF_5]$[52] and 2.577−2.609 Å for $[H_3O][BF_4]$,[53] there is ultimately nothing dramatically different and exact details on H-bonding for $[H_3O][Sb_2F_{11}]$ are found in the Supporting Information.

A stereoscopic view of the unit cell is shown in Figure 2, which illustrates the complexity of the molecular structure and the polymeric nature of $[H_3O][Sb_2F_{11}]$. As seen in Table 1, there are 24 molecules per unit cell with 3 different independent $[Sb_2F_{11}]^-$ ions labeled **a**, **b**, and **c** and shown, together with selected bond distances and bond angles in Figure 3. A detailed listing of bond parameters is found in Tables 3 (bond lengths) and 4 (bond angles). Also shown in Figure 3 are cation−anion contacts via various types of hydrogen bonds. The connectivity via O−H--F bridge bonds differs for all three anions, but the structural consequences for each anion are rather similar and are summarized below.

In the absence of any interactions, the dioctahedral anion is expected to have D_{4h} symmetry. This implies a linear $F_{ax}-Sb-F_b-Sb-F_{ax}$ chain with a symmetrical $Sb-F_b-Sb$ bridge and two eclipsed $Sb(F_{eq})_4$-planes. Both F_{eq} and F_{ax} are expected to be approximately equidistant to antimony while $Sb-F_b$ bonds are expected to be longer. In $[H_3O][Sb_2F_{11}]$ departures from expectations involve the following. (i) The $Sb-F_b-Sb$ segment is no longer linear and has bond angles ranging from 149.4(3) to 145.9(2)°. (ii) Both SbF_4 groups become staggered and are no longer strictly planar. F_{eq} atoms in both planes "lean" toward the bridging F atoms and $F_{eq}-Sb-F_b$ angles are now less, while $F_{eq}-Sb-F_{ax}$ angles are slightly more than 90° by about 3 to 5°. (iii) As some of the axial and the equatorial F atoms are involved in H-bonding, $Sb-F_{eq}$ bond distances show a wider spread. Curiously some of the shortest (1.785(7) Å) and some of the longest (1.852(5) Å) Sb−F bond distances involve F atoms engaged in hydrogen bonding and no consistent picture emerges. (iv) A very slight asymmetry of the $Sb-F_b-Sb$ bridge is found in two cases, forms **a** and **b** shown in Figure 3a,b.

The principal cause for these deviations from expectations appears to be the rather irregular interionic hydrogen bonds. It appears that the bond angle deviations (i) and (ii) are more pronounced than the changes in bond distances (iii) and (iv), which are rather subtle.

Similar deformations of the $[Sb_2F_{11}]^-$ anion have recently been noticed by us for $[Hg(CO)_2][Sb_2F_{11}]_2$[40] and, to a lesser extent for $[Ir(CO)_5Cl][Sb_2F_{11}]_2$,[42] where significant interionic Hg--F[40] and C--F[40,42] contacts take the place of H--F interactions found here for $[H_3O][Sb_2F_{11}]$. The effects of these interionic contacts on the $[Sb_2F_{11}]^-$ ions are however similar for both groups of compounds. The importance of these secondary contacts is illustrated by two observations: (a) the vast majority (8 out of 9) thermally stable homoleptic carbonyl cations of electron rich metals exist only as $[Sb_2F_{11}]^-$ salts,[4,38,40,42] and (b) some unusual, highly electrophilic cations of non-metallic main group elements are also seemingly stabilized by $[Sb_2F_{11}]^-$. Where molecular structures are known, as in salts with $[I_2]^+$,[54] $[TeF_3]^+$,[55] $[IF_4]^+$,[56] $[BrF_4]^+$,[57] $[XeF]^+$,[58] $[XeF_3]^+$,[59] $[SbCl_4]^+$,[60]

(54) Davies, C. J.; Gillespie, R. J.; Ireland, P. R.; Sowa, J. M. *Can. J. Chem.* **1974**, *52*, 2048.
(55) Edwards, A. J.; Taylor, P. *J. Chem. Soc., Dalton Trans.* **1973**, 2150.
(56) Edwards, A. J.; Taylor, P. *J. Chem. Soc., Dalton Trans.* **1975**, 2174.
(57) Lind, M. D.; Christe K. O. *Inorg. Chem.* **1972**, *11*, 608.
(58) McKee, D. E.; Adams, C. J.; Zalkin, A.; Bartlett, N. *J. Chem. Soc., Chem. Commun.* **1973**, 26.

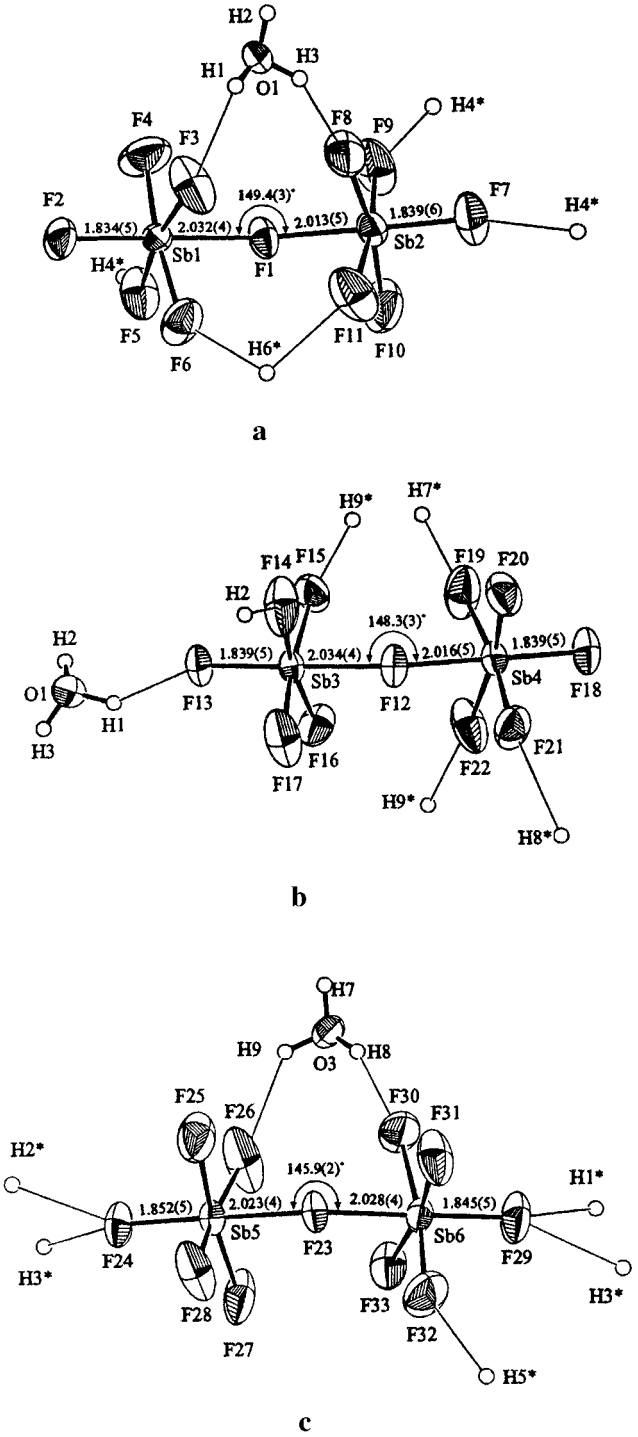

Figure 3. (a) Molecular structure of $[H_3O][Sb_2F_{11}]$ (***a***) (33% probability thermal ellipsoids are shown, bond lengths in Å). (b) Molecular structure of $[H_3O][Sb_2F_{11}]$ (***b***) (33% probability thermal ellipsoids are shown, bond lengths in Å). (c) Molecular structure of $[H_3O][Sb_2F_{11}]$ (***c***) (33% probability thermal ellipsoids are shown, bond lengths in Å).

and $[Se_2I_4]^{2+}$,[61] significant secondary interionic contacts between F of the anion and the electropositive non-metal moiety are frequently observed. Likewise salts of the fluoronium cations $[H_2F]^+$ and $[H_3F_2]^+$ with $[Sb_2F_{11}]^-$ [62] show again asymmetric interionic hydrogen bonds of the F−H--F type.

The structure of $[H_3O][Sb_2F_{11}]$ reported here and the examples quoted from our[4,38,40,42] or from other laboratories[54−62] all point to a unique role of the $[Sb_2F_{11}]^-$ anion. In addition to its very low nucleophilicity,[2,3,11] the flexibility provided by the weakly bonded Sb−F_b−Sb bridging group, facilitates the formation of significant secondary interionic contacts between the anion and various electrophilic cations, some of which exist only as $[Sb_2F_{11}]^-$ salts. Detection of these secondary contacts requires reliable and accurate molecular structure data. It is fortuitous, that the accurate ($R_w = 0.032$) molecular structure of $[H_3O][Sb_2F_{11}]$ provides three slightly different $[Sb_2F_{11}]^-$ anions.

In contrast, for cubic $[H_3O][SbF_6]$[27] interionic hydrogen bonding is manifested in a more regular distortion of the $[SbF_6]^-$ octahedron in two ways: (i) bond angles (F−Sb−F) depart from 90° and range from 84.4(3) to 95.6(4)° (ii) two pairs (three each) of Sb−F bond distances of 1.854(9) and 1.891(7) Å are reported. Interestingly, shorter Sb−F bonds and wider F−Sb−F bond angles involve F atoms engaged in the formation of asymmetric hydrogen bonds to oxygen of the oxonium cation. Longer Sb−F bonds (1.891(7) Å) and slightly more acute F−Sb−F bond angles are observed for F atoms involved only in "nonbonded contacts" with oxygen of the cation.

Even though Sb−F distances in $[H_3O][Sb_2F_{11}]$ are more irregular and cover a wider range (1.785(7)−1.852(5) Å) than in $[H_3O][SbF_6]$,[27] they are in general shorter than the two Sb−F bond distances (1.854(9) and 1.891(7) Å) in $[H_3O][SbF_6]$.[27] In the two related oxonium salts, tighter bonding to the peripheral F atoms in $[Sb_2F_{11}]^-$ than in $[SbF_6]^-$ suggests that the former should be a weaker nucleophile than $[SbF_6]^-$. Whether this is generally true is difficult to decide, because structurally characterized pairs of $[SbF_6]^-$ and $[Sb_2F_{11}]^-$ salts with a common cation such as $[H_3O][SbF_6]$[26,27] and $[H_3O][Sb_2F_{11}]$ appear to be uncommon.

(ii) $CsSO_3F$ (2) and $Cs[H(SO_3F)_2]$ (3). As in the preceding section, a pair of salts with a common cation, in this case Cs^+, and two related anions, mononuclear $[SO_3F]^-$ and dinuclear $[H(SO_3F)_2]^-$, are discussed and compared. The place of the fluorine bridge in $[Sb_2F_{11}]^-$ is in dinuclear $[H(SO_3F)_2]^-$ taken by a bridging proton. In addition to the internal bond parameters of the two fluorosulfato anions and the relationship of these parameters to the nucleophilicity of the two superacid anions derived from HSO_3F, interionic contacts to Cs^+ will be discussed. It is recognized that these contacts to the very weak electrophile Cs^+ will be rather long and weak. As more electrophilic, molecular cations are encountered, these interionic contacts are expected to shorten and to increase in strength. At present the structures discussed here may indicate trends in the coordinating ability of superacid anions, as the peripheral atoms of the anions change from F only in the fluoroantimonates to O and F in the fluorosulfate derivatives discussed here and in the subsequent section.

The molecular structures and the coordination environments of the cations for $CsSO_3F$ and $Cs[H(SO_3F)_2]$ are shown in Figures 4 and 5, respectively together with selected bond parameters for both salts. A more detailed listing of bond lengths and angles is found in Tables 3 and 4. In the case of $CsSO_3F$, the bond parameters are compared in Table 5 to the previously reported corresponding data for $LiSO_3F$,[28] KSO_3F,[29] and NH_4SO_3F,[30] which for $LiSO_3F$ are affected by the strongly polarizing, tetrahedrally coordinated Li^+ cation. In the structures of KSO_3F[29] and to a lesser degree of NH_4SO_3F,[30] anion disorder involving O and F atoms is encountered.

The monoclinic space group $P2_1/a$ determined by us for $CsSO_3F$ differs from conclusions arrived at in an earlier study,[31] where the crystal structure of $CsSO_3F$ is determined by

(59) McRae, V. M.; Peacock, R. D.; Russell, D. R. *J. Chem. Soc., Chem. Commun.* **1969**, 62.
(60) Miller, H. B.; Baird, H. W.; Bramlett, C. L.; Templeton, W. K. *J. Chem. Soc., Chem. Commun.* **1972**, 262.
(61) Nandana, W. A. S.; Passmore, J.; White, P. S.; Wong, C.-M. *Inorg. Chem.* **1990**, *29*, 3529.
(62) Mootz, D.; Bartmann, K. *Angew Chem., Int. Ed. Engl.* **1988**, *27*, 391.

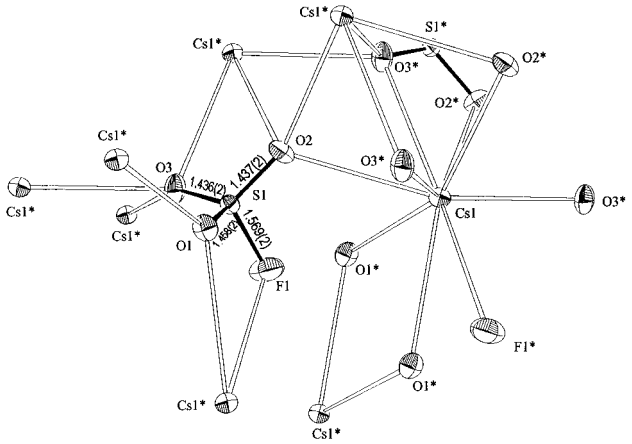

Interatomic distances (Å):

S1-F1	1.569(2)	F1-Cs*	3.252(2)	S1-O1	1.458(2)	O1-Cs*	3.329(2)
						O1-Cs*	3.220(2)
S1-O2	1.437(2)	O2-Cs*	3.223(3)	S1-O3	1.436(2)	O3-Cs*	3.151(2)
		O2-Cs*	3.265(2)			O3-Cs*	3.316(3)
		O2-Cs*	3.115(2)			O3-Cs*	3.119(2)

Selected bond angles (°):

∠F1-S1-O1	102.3(1)°	∠F1-S1-O2	106.3(1)°	∠F1-S1-O3	107.8(1)°
∠O1-S1-O3	112.7(1)°	∠O1-S1-O2	113.6(1)°	∠O2-S1-O3	113.2(1)°

Figure 4. Structure of $CsSO_3F$ (33% probability thermal ellipsoids are shown).

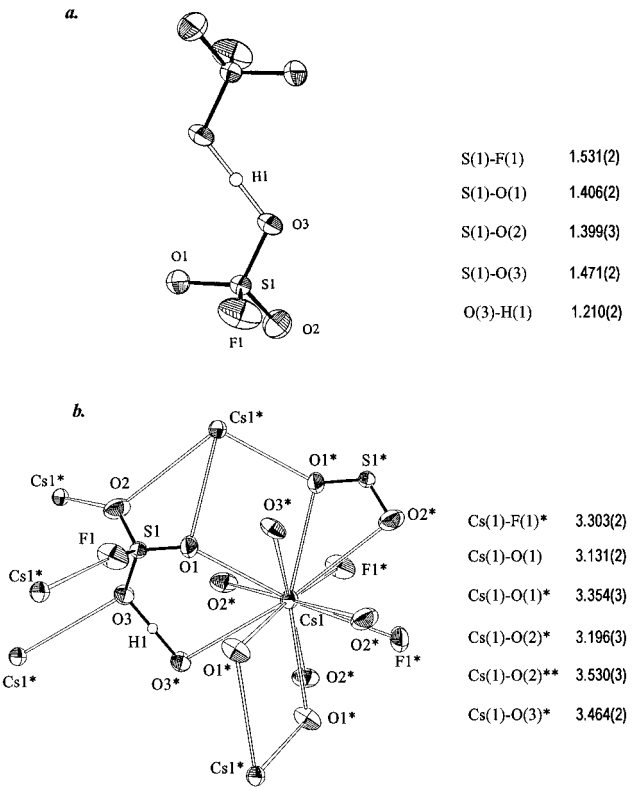

Figure 5. Structure of $Cs[H(SO_3F)_2]$ (33% probability thermal ellipsoids are shown; bond distances in Å): (a) $H(SO_3F)_2^-$ ion; (b) coordination environment of the Cs^+ ion.

macrocrystallography and by the use of powder diffraction data. Here the suggested space group is $I4_1/a$ (C^6_{4h}) and O and F disorder is observed. It is conceivable that $CsSO_3F$ shows polymorphism and crystallizes in two or more different forms, even though here and previously[31] an identical synthetic procedure and recrystallization from water are used to obtain suitable crystals for the structure determinations.

Table 5. Structural Parameters of the Fluorosulfate Anion in Alkali Metal Fluorosulfates and NH_4SO_3F

	compound			
structure param	$LiSO_3F$[28]	KSO_3F[29]	NH_4SO_3F[30]	$CsSO_3F$[a]
bond length (Å)				
S−O(1)	1.455(6)			1.458(2)
S−O(2)	1.424(4)	1.43(1)	1.45(2)	1.437(2)
S−O(3)	1.424(4)			1.436(2)
S−F	1.555(7)	1.57(2)	1.55(2)	1.569(2)
bond angle (deg)				
F(1)-S−O(1)	104.5(5)			102.3(1)
F(1)-S−O(2)	102.8(3)	105.8(7)	106(1)	106.3(1)
F(1)-S−O(3)	102.8(3)			107.8(2)
O(1)-S−O(2)	113.5(2)			113.6(1)
O(1)-S−O(3)	113.5(2)	112.9(7)	113(1)	113.2(1)
O(2)-S−O(3)	117.4(4)			112.7(1)

[a] This work.

Crystal data and unit cell dimensions obtained for $Cs[H(SO_3F)_2]$ agree reasonably well with those reported previously in a preliminary communication.[14] The reliability of the molecular structure determination has improved slightly, judging by the R value of 0.027 vs 0.04.[14] The presence of a symmetrical, linear hydrogen bridge is confirmed and the hydrogen atom is located. The O−H distance of 1.210(2) Å is in agreement with the previously reported[14] O--O distance of 2.41(1) Å. As seen in Tables 3 and 4 and Figure 5, complete bond parameters are obtained and the coordination environment of Cs^+ is now apparent.

For $CsSO_3F$, as seen in Figure 4, the fluorosulfate anion appears to depart very slightly from C_{3v} symmetry toward the point group C_s. The distance of sulfur to O(1), which has two nearest Cs^+ neighbors, is 1.458(2) Å, very slightly longer than the other two S−O distances, which are 1.437(2) and 1.436(2) Å, identical within estimated standard deviations. A further slight nonequivalency is caused by weak interionic contacts to Cs^+. While O(1) has two contacts as mentioned, the remaining two O atoms have three contacts each at comparable distances of 3.115(2)−3.329(2) Å. Adding to these a single F--Cs^+ contact of 3.252(2) Å indicates that the cation in $CsSO_3F$ is nine coordinate, with eight sites occupied by oxygen and one by fluorine.

The suggested reduction in symmetry of the SO_3F^- group in $CsSO_3F$ is consistent with the Raman spectrum, obtained on single crystalline material. In the spectral range of the internal vibrations due to the fluorosulfate ion, the three E-modes, expected for point group C_{3v}, are very slightly split into two components by 11−24 cm^{-1}.

Considerably larger splittings of the E-modes are reported for $LiSO_3F$.[63] According to the molecular structure,[28] nonequivalence is caused by small differences in S−O bond length and by coordination to the Li^+ cation, which achieves an approximately tetrahedral environment by interacting singly with Li--O 1.903(10) Å with two O atoms and doubly at 2.045 Å with the third oxygen of the fluorosulfate group. Interestingly, the fluorosulfate ion in KSO_3F has, according to its vibrational spectrum[63,64] strict C_{3v} symmetry, even though this is not clearly confirmed by the molecular structure determination on account of disorder problems[29] which also affect the structural study of NH_4SO_3F.[30]

As seen in Table 5, all observed bond distances and bond angles for $CsSO_3F$ fall into the expected range. For $LiSO_3F$[28]

(63) Ruoff, A.; Milne, J. B.; Kaufmann, G.; Leroy, M. *Z. Anorg. Allg. Chem.* **1970**, *372*, 119.
(64) Goubeau, J.; Milne, J. B. *Can. J. Chem.* **1967**, *45*, 2321.

some of the corresponding distances are very slightly shorter. Comparable bond parameters are also found for KSO_3F[29] and NH_4SO_3F,[30] but large standard deviations cause some uncertainty.

The formal addition of one mole of fluorosulfuric acid to $CsSO_3F$ results in the formation of a monosolvate of the composition $Cs[H(SO_3F)_2]$ and causes structural changes. The presence of a rather short O--H--O hydrogen bond (O--O = 2.420(2) Å), has been the subject of a preliminary communication by others[14] and little needs to be added at this time. With the H atom found at an inversion center, the O--H--O bond is indeed linear and symmetrical as claimed.[14]

On account of the hydrogen bond formation, the corresponding S−O bonds are lengthened to 1.471(2) Å and the remaining S−O bonds (1.399(3) and 1.406(2) Å) and the S−F bond (1.531(2) Å) are shortened relative to the bond distances of $CsSO_3F$ as seen in Figure 5. As noted previously for Sb−F distances of the pair $[SbF_6]^-$ and $[Sb_2F_{11}]^-$ with $[H_3O]^+$ as cation,[27] bonding to the peripheral F atoms or to O and F in the pair SO_3F^- and $[H(SO_3F)_2]^-$ strengthens for the dinuclear species at the expense of the bond strength in the bridging region. While $Sb-F_{ax}$, and $Sb-F_{eq}$ bond shortening in $[Sb_2F_{11}]^-$ is somewhat obscured by interionic, asymmetric hydrogen bonding, which results in a spread of Sb−F bond distances as discussed, a clearer situation is encountered for $CsSO_3F$ and $Cs[H(SO_3F)_2]$. Only rather regular, long and weak interionic contacts to Cs^+ are observed for the latter which do not appear to affect internal bonds of the anion $[H(SO_3F)_2]^-$. As seen in Figure 5, the four peripheral O atoms of the anion are 2-fold coordinated to Cs^+, while both F and even the 2-fold coordinated O atoms in the O-H-O bridge link singly to Cs^+. This results in a coordination number of 12 for cesium, which is not uncommon. Cs^+--O(F) contacts range from 3.131(2) to 3.530(3) Å and appear to be slightly longer than contacts found for $CsSO_3F$ (3.115(2)−3.329(2) Å). As S−O and S−F bonds involving peripheral atoms strengthen slightly from $CsSO_3F$ to $Cs[H(SO_3F)_2]$, the basicity of the peripheral atoms decreases and the ability of these atoms to coordinate to Cs^+ is seemingly reduced. In summary, of the two superacid anions in the Brönsted superacid HSO_3F, the fluorosulfate ion SO_3F^- appears to be a slightly stronger nucleophile than its monosolvate $[H(SO_3F)_2]^-$, just as $[SbF_6]^-$ appears to be more basic than $[Sb_2F_{11}]^-$ in the pair of $[H_3O]^+$ salts, discussed in the preceding section. More extensive electron delocalization in the dinuclear anions $[H(SO_3F)_2]^-$ and $[Sb_2F_{11}]^-$ results in lower nucleophilicity relative to the mononuclear anions SO_3F^- and $[SbF_6]^-$.

(iii) $Cs[Au(SO_3F)_4]$ (4), $Cs_2[Pt(SO_3F)_6]$ (5), and $Cs[Sb(SO_3F)_6]$ (6). A simple rationale links the dinuclear Brönsted anion $[H(SO_3F)_2]^-$ to the three anions discussed in this section. All belong to existing[6,18] or potential[15] homoleptic conjugate superacid systems in fluorosulfuric acid. In all four anions a central monoatomic, hypothetical cation M^{n+} (e.g. H^+, Au^{3+}, Pt^{4+}, Sb^{5+}), acts as a strong Lewis acid. Increasing numbers (2,4, or 6) of the fluorosulfate anions are coordinated in pairs via oxygen to give uninegative ($[H(SO_3F)_2]^-$, $[Au(SO_3F)_4]^-$, and $[Sb(SO_3F)_6]^-$) or dinegative ($[Pt(SO_3F)_6]^{2-}$) superacid anions. The resulting coordination geometries are expected to be linear ($[H(SO_3F)_2]^-$), square planar ($[Au(SO_3F)_4]^-$), or octahedral ($[Pt(SO_3F)_6]^{2-}$, $[Sb(SO_3F)_6]^-$). The strength of the cation−fluorosulfate interaction will be reflected directly in short and strong bonds between the central cation and the O_b atoms of the singly coordinated fluorosulfate groups. Since the four centers have different ionic radii due to discrepancies in atomic number and ionic charge, the resulting $M-O_b$ bond distances are not strictly comparable. Strong coordination of the fluorosulfate groups via oxygen to the central ion will have two indirect, secondary effects, which will be comparable within the group of the four anions: (i) the bond of sulfur to the bridging oxygen O_b will lengthen and (ii) as discussed above for $[H(SO_3F)_2]^-$, due to increased multiple bonding in the approximately tetrahedral fluorosulfate group, the bonds of sulfur to the peripheral O and F atoms will shorten, relative to S−O and S−F bond distances in $CsSO_3F$. Both indirect effects will be proportional to the intrinsic Lewis acidity of the central cation M^{n+} and will determine the nucleophilicity of the polyfluorosulfato anion.

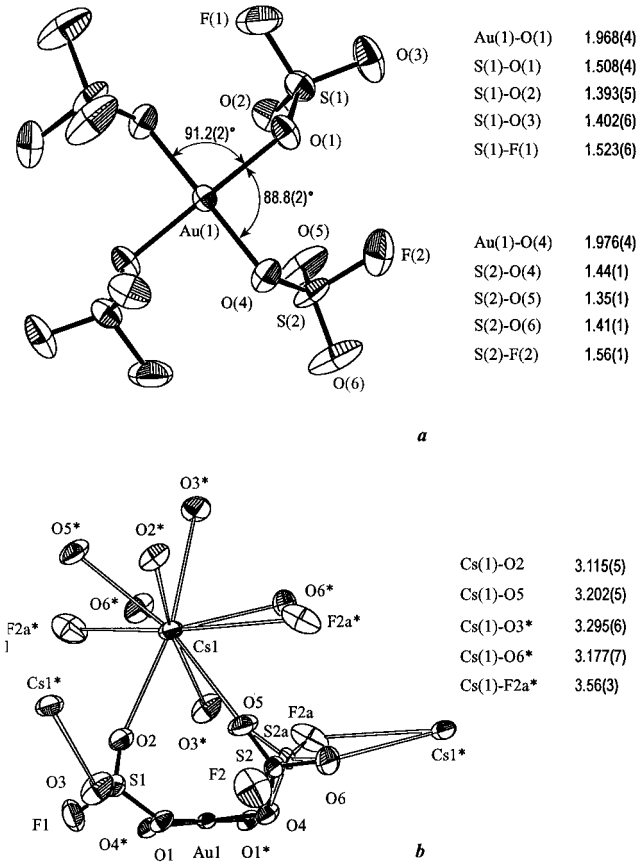

Au(1)-O(1)	1.968(4)
S(1)-O(1)	1.508(4)
S(1)-O(2)	1.393(5)
S(1)-O(3)	1.402(6)
S(1)-F(1)	1.523(6)
Au(1)-O(4)	1.976(4)
S(2)-O(4)	1.44(1)
S(2)-O(5)	1.35(1)
S(2)-O(6)	1.41(1)
S(2)-F(2)	1.56(1)

Cs(1)-O2	3.115(5)
Cs(1)-O5	3.202(5)
Cs(1)-O3*	3.295(6)
Cs(1)-O6*	3.177(7)
Cs(1)-F2a*	3.56(3)

Figure 6. Structure of $Cs[Au(SO_3F)_4]$ (33% probability thermal ellipsoids are shown; bond lengths in Å): (a) $[Au(SO_3F)_4]^-$ ion (disorder of the S(2) fluorosulfate group is not shown); (b) coordination environment of the Cs^+ ion in $Cs[Au(SO_3F)_4]$.

Expected trends in internal bond distances of the superacid anions will be affected and possibly slightly modified by interionic contacts to the cation Cs^+. The molecular structures of $Cs[Au(SO_3F)_4]$, $Cs_2[Pt(SO_3F)_6]$ and of $Cs[Sb(SO_3F)_6]$, including the respective coordination environments of Cs^+ are shown in Figures 6−8. Included in the figures are selected bond distances and interionic contacts to Cs^+. More detailed bond lengths and distances are found in Table 3. Bond angles for all three salts are found in Table 4.

As seen in Figure 6, the coordination environment for gold in the $[Au(SO_3F)_4]^-$ anion is approximately square planar, consistent with a $5d^8$ electron configuration for Au(III). The O−Au−O bond angles of 88.8(2) and 91.2(2)° depart very slightly from 90°. The anion $[Au(SO_3F)_4]^-$ has C_i symmetry: two adjacent SO_2F groups point upward out of the AuO_4-plane and the two remaining ones point downward. Similar conformations are found for the anion $[Au(NO_3)_4]^-$ [34] and the neutral, dimeric molecule $[Au(SO_3F)_3]_2$.[35] The Au−O bond distances average 1.972(4) Å and are slightly shorter than in $[Au(NO_3)_4]^-$ [34] (2.03(2) and 1.99(1) Å) and in $[Au(SO_3F)_3]_2$[35] (2.018(6) and 1.958(8) Å). In the latter compound, the presence of terminal,

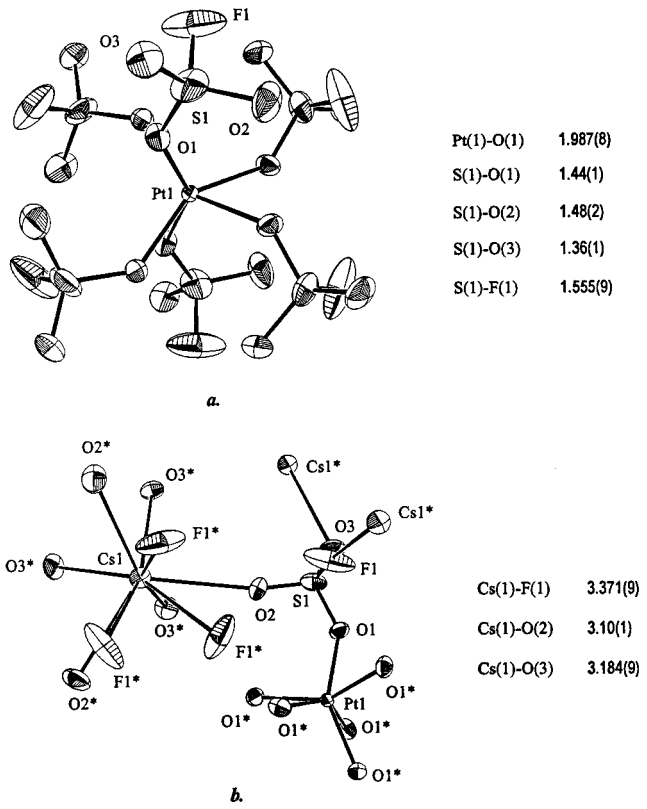

Figure 7. Structure of $Cs_2[Pt(SO_3F)_6]$: (a) $[Pt(SO_3F)_6]^{2-}$ ion; (b) environment of the Cs^+ ion (33% probability thermal ellipsoids are shown; bond lengths in Å).

monodentate and bridging, bidentate fluorosulfate groups causes some distortion and a wider spread of Au−O distances (see above) and bond angles (87.4(3)−93.2(3)°). However as the two average Au−O bond distances of 1.972(4) Å for $[Au(SO_3F)_4]^-$ and 1.988(7) Å for $[Au(SO_3F)_3]_2$[35] indicate, the formal addition of two SO_3F^- ions to the Lewis acid $[Au(SO_3F)_3]_2$ to produce the anion $[Au(SO_3F)_4]^-$, with retention of the square planar coordination geometry, does not result in a lengthening but rather in a slight contraction of the averaged Au−O bonds of the anion. Consequently sulfur bond distances to the coordinated oxygen O_b in the anion are slightly longer than in the neutral molecule.[35] However there are two interesting differences between neutral $[Au(SO_3F)_3]_2$[35] and $[Au(SO_3F)_4]^-$: in the dimer extensive thermal motion of the peripheral atoms of terminal fluorosulfate groups causes difficulties in the exact determination of S−O and S−F bond distances for the peripheral atoms. In addition, significant intermolecular contacts between gold and peripheral O atoms from adjacent layers of $[Au(SO_3F)_3]_2$ molecules are noted. In $Cs[Au(SO_3F)_4]$ interlayer contacts are not observed and thermal motion of the $-SO_2F$ moieties appears to be suppressed. The observed interionic contacts between Cs^+ and peripheral O and F atoms of the anion appear to replace interlayer interactions and restrict or quench thermal motions of the $-SO_2F$ groups. The 10-coordinate Cs^+ ion in $Cs[Au(SO_3F)_4]$ has eight relatively short (3.115(5) to 3.295(5) Å) contacts to oxygen and two longer (3.56(3) Å) contacts to fluorine. A discussion of the rather short S−O and S−F distances will be deferred for the moment and a comparison of these distances for all four anions in this group will be presented later.

In $Cs_2[Pt(SO_3F)_6]$, the expected octahedral coordination polyhedron about platinum is trigonally distorted (rotation about one of the C_3 axes) and is in fact more nearly a trigonal prismatic coordination geometry with crystallographic D_3 and approximate D_{3h} symmetry. Such distortions are unusual for complexes with monodentate ligands such as the fluorosulfate groups. Furthermore, complexes of Pt(IV) with a $5d^6$ electron configuration are expected and generally found to be octahedral. The only discernible reason for the observed distortion of the $[Pt(SO_3F)_6]^{2-}$ anion appears to be significant interionic contacts. As seen in Figure 7, the Cs^+ cation is 9-coordinate. The six Cs--O bond distances of 3.10(1) and 3.184(9) Å are among the shortest encountered in this study. Three longer Cs--F contacts of 3.371(9) Å complete the coordination sphere of Cs^+, which has exact C_3 symmetry.

As in the case of $[H_3O][Sb_2F_{11}]$ (vide supra) or of $[Hg(CO)_2][Sb_2F_{11}]_2$,[40] interionic contacts either via asymmetric hydrogen bonds or via weak fluorine bridges to electropositive atoms (Hg and C) of the linear $[Hg(CO)_2]^{2+}$ cation appear to be accompanied by significant distortions of the anions. For a mononuclear anion like $[Pt(SO_3F)_6]^{2-}$, a rotational distortion appears to be most effective to allow strong contacts to Cs^+. In addition the net charge of −2 may suggest a slightly higher anion basicity resulting in higher electron density on the peripheral atoms. Unfortunately the structure of $Cs_2[Pt(SO_3F)_6]$ is of poorer quality ($R_w = 0.045$) than those of the other salts discussed here. Larger estimated standard deviations appear to affect bond parameters of the fluorosulfate groups, so that a comparison is difficult. Consistent with the use of platinum(IV) fluorosulfate as Lewis acid in the $HSO_3F-Pt(SO_3F)_4$[18] system, the Pt−O distance of 1.987(8) Å is rather short.

By contrast the final molecular structure in this series, that of $Cs[Sb(SO_3F)_6]$, is rather regular. The six symmetry related fluorosulfate groups are octahedrally coordinated to antimony, and as seen in Figure 8 the resulting $[Sb(SO_3F)_6]^-$ anion has exact S_6 symmetry. Again the Sb−O distance (1.955(2) Å) is short and of the same order of magnitude as M−O distances in the previously discussed superacid anions $[Au(SO_3F)_4]^-$ and $[Pt(SO_3F)_6]^{2-}$.

Slightly shorter Sb−O distances are reported[36] for $[Sb(OTeF_5)_6]^-$ (1.91(1) to 1.96(1) Å, which also has antimony in an octahedral coordination environment but crystallizes with either $[N(CH_3)_4]^+$ or $[N(C_2H_5)_4]^+$ as cation in two slightly different forms). Interestingly the related salt $[N(CH_3)_4][As(OTeF_5)_6]$ has the same space group ($R\bar{3}$) as $Cs[Sb(SO_3F)_6]$.

The cesium ion is 12-coordinate but the weak interionic contacts involve only both peripheral oxygen atoms of each SO_3F group and not fluorine. Two Cs--O contacts of 3.241(3) and 3.413(4) Å are found and the resulting polyhedron may be viewed as a regularly distorted dodecahedron. The Cs^+ ion has exact crystallographic C_3 symmetry.

The coordination environments of Cs^+ are summarized in Table 6 for all five salts studied here. As can be seen the coordination number 9 is found for $CsSO_3F$ and $Cs_2[Pt(SO_3F)_6]$. For $CsSO_3F$, oxygen is doubly and triply coordinated to different Cs^+, while F is singly coordinated (see Figure 10). In $Cs[Au(SO_3F)_4]$ the coordination number increases to 10; however, interionic contacts involving F are rather long. Finally, coordination number 12 is achieved for $Cs[H(SO_3F)_2]$ where peripheral O atoms are doubly coordinated while fluorine and bridging oxygen are singly coordinated and contacts are rather long, and for $Cs[Sb(SO_3F)_6]$, where only oxygen is very weakly coordinated to Cs^+. The resulting coordination polyhedron is the most regular of the five polyhedra about Cs^+ observed in this study, and the $[Sb(SO_3F)_6]^-$ ion is the least coordinating anion of the five studied here.

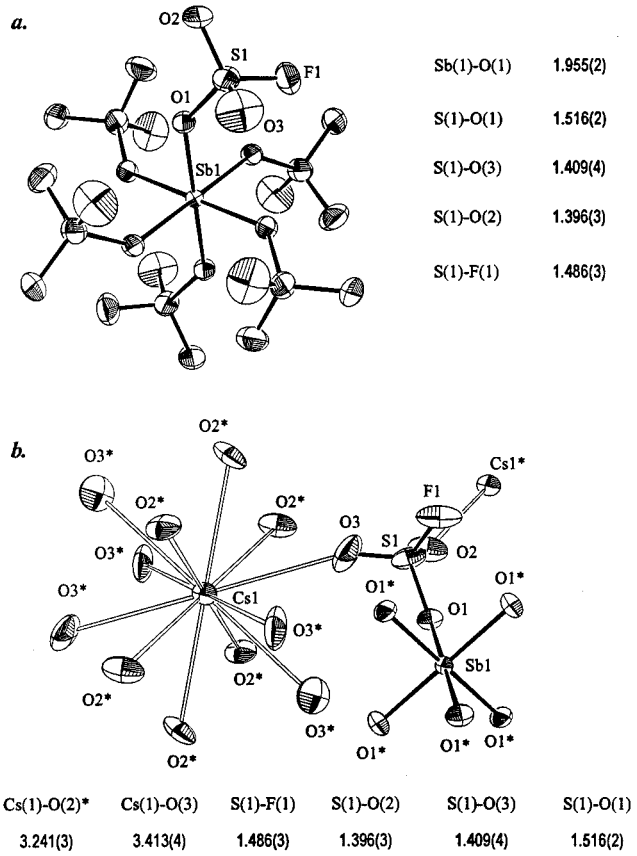

Figure 8. Structure of $Cs[Sb(SO_3F)_6]$: (a) $[Sb(SO_3F)_6]^-$ ion; (b) environment of the Cs^+ ion (33% probability thermal ellipsoids are shown; bond lengths in Å).

Table 6. Coordination Environment of Cs^+ in Cesium Salts of Superacid Anions

		Cs···O contacts		Cs···F contacts	
compounds	coord no.	no.	interatomic dist, Å	no.	interatomic dist, Å
$CsSO_3F$	9	8	3.115−3.265	1	3.252
$Cs[H(SO_3F)_2]$	12	10	3.131−3.530	2	3.303
$Cs[Au(SO_3F)_4]$	10	8	3.115−3.295	2	3.56
$Cs_2[Pt(SO_3F)_6]$	9	6	3.10−3.184	3	3.371
$Cs[Sb(SO_3F)_6]$	12	12	3.241 (×6) 3.413 (×6)		

It may be argued that it is inappropriate to talk about "coordination" with bond distances between 3.1 and 3.56 Å. Our use of the coordination concept is based on crystallographic criteria as applied to ionic compounds. Here coordination number is defined as the number of nearest neighbor atoms. The weak interionic contacts observed here are not to be confused with coordinate bonds in classical coordination compounds. Nevertheless a number of interesting conclusions can be reached based on the five structures of the Cs^+ salts reported here: (i) Peripheral atoms of the molecular anion are most likely to coordinate to the cation. (ii) The F atom of a fluorosulfate group is less likely to coordinate to Cs^+ than are the oxygen atoms, even though both are often peripheral atoms. This can be readily explained by the use of electronegativity arguments where F is more electronegative than O and conversely less basic. An illustration of this observation is found in the molecular structures of *cis*-$Pt(CO)_2(SO_3F)_2$[65] and of *mer*-$Ir(CO)_3(SO_3F)_3$[41] obtained by us, where inter- and intramolecular contacts to the C atom of the CO group involve only O but not F of the fluorosulfate group. (iii) Weak interionic contacts may cause distortions of the anion from expected, idealized geometries. (iv) Interionic interactions may affect and probably slightly weaken internal bonds of sulfur to peripheral atoms. This latter point will be discussed in more detail below, where relevant features of the fluorosulfato anions are compared.

B. A Comparison of the Fluorosulfato Superacid Anions. There are two points of interest in a structural comparison of the fluorosulfate containing superacid anions: (i) the central $M-(OS-)_n$ segment for M = H, Au, Pt, or Sb and n = 2, 4, or 6, respectively, and (ii) the internal bond parameters of the O-bonded, monodentate fluorosulfate group with special emphasis on S−O and S−F bonds involving peripheral atoms. Little needs to be said here about bond angles within the fluorosulfate groups which are listed in Table 4 and in part shown in Figure 9. They deviate slightly from tetrahedral angles but comply with the VSEPR concepts of molecular geometry.[66,67] The discussion is expanded to include two other tetrahedral sulfur oxygen species, the fluorosulfate ion in $CsSO_3F$ (vide supra) and gaseous sulfuryl fluoride SO_2F_2, where data from an electron diffraction study are considered.[68] This molecule is frequently[69] claimed to have the shortest S−O and S−F bonds found in neutral, tetrahedrally coordinated sulfur−oxygen−fluorine compounds.

The bond parameters for the central section of the four anions $[H(SO_3F)_2]^-$, $[Au(SO_3F)_4]^-$, $[Pt(SO_3F)_6]^{2-}$ and $[Sb(SO_3F)_6]^-$ are all listed in Table 7. Also included are S−O and S−F bond distances of the peripheral atoms. Data for the SO_3F-moiety in $[Pt(SO_3F)_6]^{2-}$ are as discussed, rather inaccurate and are listed here for completeness. In Figure 9 idealized structures of the SO_3F group in all four anions, in SO_3F^-, and in SO_2F_2[68] are presented. Bond distances in Å are included in the drawings and selected bond angles appear above each structural drawing.

In addition to the short $M-O_b$ distances which have been discussed already and the subsequent lengthening of the O_b-S bonds, which follows the order $[H(SO_3F)_2]^- < [Au(SO_3F)_4]^- < [Sb(SO_3F)_6]^-$, the bond angle $M-O_b-S$, M = H, Au, Pt, or Sb, is of interest. As the coordination number of M increases, this angle widens from 117.1(2)° for $[H(SO_3F)_2]^-$ over 125.2(3)° for $[Au(SO_3F)_4]^-$ to nearly identical angles of 135.3(7) and 136.6(1)° for $[Pt(SO_3F)_6]^{2-}$ and $[Sb(SO_3F)_6]^-$ respectively. Similar wide $M-O_b-Te$ angles of ∼135−137° are found for $[M(OTeF_5)_6]^-$, M = Bi, while the corresponding Sb complexes show the widest angles, which range up to 167°, about 30° wider than those found for $[Sb(SO_3F)_6]^-$. This increase appears to argue against steric repulsion between stereochemically demanding $OTeF_5$ groups as a cause of the widening of the M−O−Te angles as had been claimed previously,[70] based on the molecular structures of neutral species $M(OTeF_5)_6$, M = Te, Mo, or U. Steric repulsion should decrease with increasing atomic number and size of the central atom, but the opposite is found for the $[M(OTeF_5)_6]^-$ anions.[36]

Alternatively an increase in M−O bond strength can be considered as cause for angle widening which may involve delocalization of lone pair electron density from the bridging oxygen to M and to S. The trend apparent in Table 7 is in agreement with this assumption, since for M = H the most acute angle is observed and the angle widening increases with the increasing oxidation state of M.

(65) Wang, C.; Willner, H.; Bodenbinder, M.; Batchelor, R. J.; Einstein, F. W. B.; Aubke F. *Inorg. Chem.* **1994**, *33*, 3521.
(66) Gillespie, R. J. *The VSEPR Model of Molecular Geometry*; Van Nostrand Reinhold: London, 1972.
(67) Gillespie, R. J.; Hargittai, I. *The VSEPR Model of Molecular Geometry*; Allyn and Bacon: Boston, 1991.
(68) Hagen, K.; Cross, V. R.; Hedberg, K. *J. Mol. Struct.* **1978**, *44*, 187.
(69) Gillespie, R. J.; Robinson, E. A. *Can. J. Chem.* **1963**, *41*, 2074.
(70) Turowsky, L.; Seppelt, K. *Z. Anorg. Allg. Chem.* **1990**, *590*, 23.

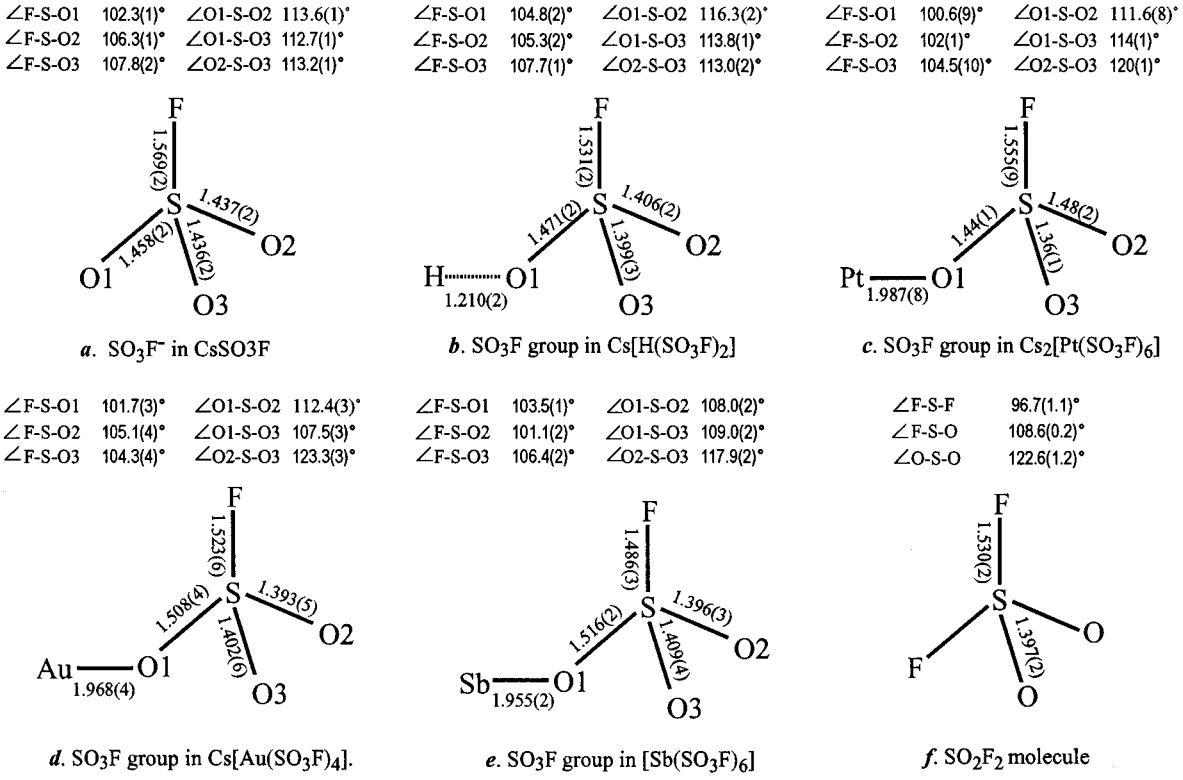

Figure 9. Structural comparison of SO_3F groups in superacid anions (bond lengths in Å).

More intriguing is the observed shortening of S−O and S−F bonds involving peripheral atoms (see Figure 9). The most striking example is the S−F distance of 1.486(3) Å in the anion $[Sb(SO_3F)_6]^-$ which is, to our knowledge, the shortest distance reported for any neutral or anionic sulfur−fluorine or sulfur−oxygen−fluorine compound, even shorter than in SO_2F_2[68] (1.530(2) Å). Only for the SOF_3^+ cation[71] are shorter S−F and S−O distances of 1.44(1) and 1.35(1) Å, respectively, reported. The S−O distances for $[Sb(SO_3F)_6]^-$ of 1.409(4) and 1.397(2) Å are comparable to the short S−O distances of gaseous SO_2F_2, 1.396(3) Å, even though interionic contacts between peripheral O atoms and Cs^+ may cause a very slight lengthening of the S−O bond in $Cs[Sb(SO_3F)_6]$.

The absence of such contacts between F and Cs^+ in $[Sb(SO_3F)_6]^-$ may contribute to the short S−F distances. For all other superacid anions listed in Table 3 and shown in Figure 9 slightly longer S−F distances are found. In all cases significant F--Cs^+ contacts are found. Hence for $[Sb(SO_3F)_6]^-$ an unusual and, in our view, unprecedented situation for a fluorosulfate species is encountered, where a S−F distance (1.486(3) Å) is measurably shorter than a sulfur−oxygen bond distance (S−O_b 1.516(2) Å) in the same molecule.

For the remaining superacid anions similar short S−O and S−F distances for the peripheral atoms are observed. For $[H(SO_3F)_2]^-$ and $[Au(SO_3F)_4]^-$ they are comparable to the corresponding distances of SO_2F_2.[68] The commonly held view, that anions should for identical groups have longer bonds than the corresponding, structurally related neutral species, is seemingly not applicable to the superacid anions, even though it applies to the isoelectronic pair SO_2F_2 and SO_3F^- (see Figure 9). Even here differences are rather small if one considers that SO_2F_2(g) is obviously an isolated molecule, while the fluorosulfate ion in solid $CsSO_3F$ is involved in interionic contacts to Cs^+, which involve both oxygen and fluorine (see Figure 4).

It seems that in approximately tetrahedral (sp^3-hybridized) sulfur(VI) compounds with small, electron rich atoms (mainly N, O or F) an excess of net negative charge contributes to an increase in multiple bonding. A striking example is provided by two, recently reported, related compounds:[72] Deprotonation of the gasphase superacid[73] $(CF_3SO_2)_2NH$ to give the anion $(CF_3SO_3)N^-$ involves an S−N bond shortening of about 0.07 Å.[72] For another pair, $[Au(SO_3F)_3]_2$[35] and $Cs[Au(SO_3F)_4]$, comparable short S−O and S−F bond distances of the terminal fluorosulfate groups to the ones in $[Au(SO_3F)_4]^-$ seem to be present but extensive thermal motion of monodentate SO_3F groups of gold(III) fluorosulfate clouds the issue.

No matter how one chooses to describe and interpret the bonding within the approximately tetrahedral, O-monodentate fluorosulfate groups, bond distances observed for all S−O and S−F groups suggest very strong multiple bonds. For $[Sb(SO_3F)_6]^-$, the most prominent example in this group, an "onion skin" model may be used to illustrate the very low basicity of this highly symmetrical superacid anion: the inner coordination sphere consists of six, octahedrally arranged O_b atoms, strongly bonded to pentavalent antimony at the core; the intermediate sphere contains six sulfur atoms again very strongly bonded to the inner sphere O_b atoms with rather wide Sb−O_b−S angles of 136.6(1)°; finally the outermost, third sphere contains 18 hard donor atoms, two groups of six O atoms and a group of six F atoms with all three groups arranged in an antiprismatic fashion. The peripheral atoms (O and F) are even more strongly bonded to sulfur than are the O atoms of the inner sphere.

In spite of strong multiple bonds, which pull the peripheral atoms toward the core, internuclear separations between O and F atoms within the outer sphere range from 2.987(6) Å for F--F

(71) Lau, C.; Lynton, H.; Passmore, J.; Siew, P.-Y. *J. Chem. Soc., Dalton Trans.* **1973**, 2535.

(72) Haas, A.; Klare, Ch.; Betz, P.; Bruckmann, J.; Krüger, C.; Tsay, Y.-H.; Aubke, F. *Inorg. Chem.* **1996**, *35*, 1918.

(73) Koppel, I. A.; Taft, R. W.; Anvia, F.; Zhu, S.-Z.; Hu, L.-Q.; Sung, K.-S.; DesMarteau, D. D.; Yagupolskii, L. M.; Yagupolskii, Y. L.; Ignat'ev, N. V.; Kondratenko, N. V.; Volkonskii, A. Y.; Vlasov, V. M.; Notario, R.; Maria, P.-C. *J. Am. Chem. Soc.* **1994**, *116*, 3047.

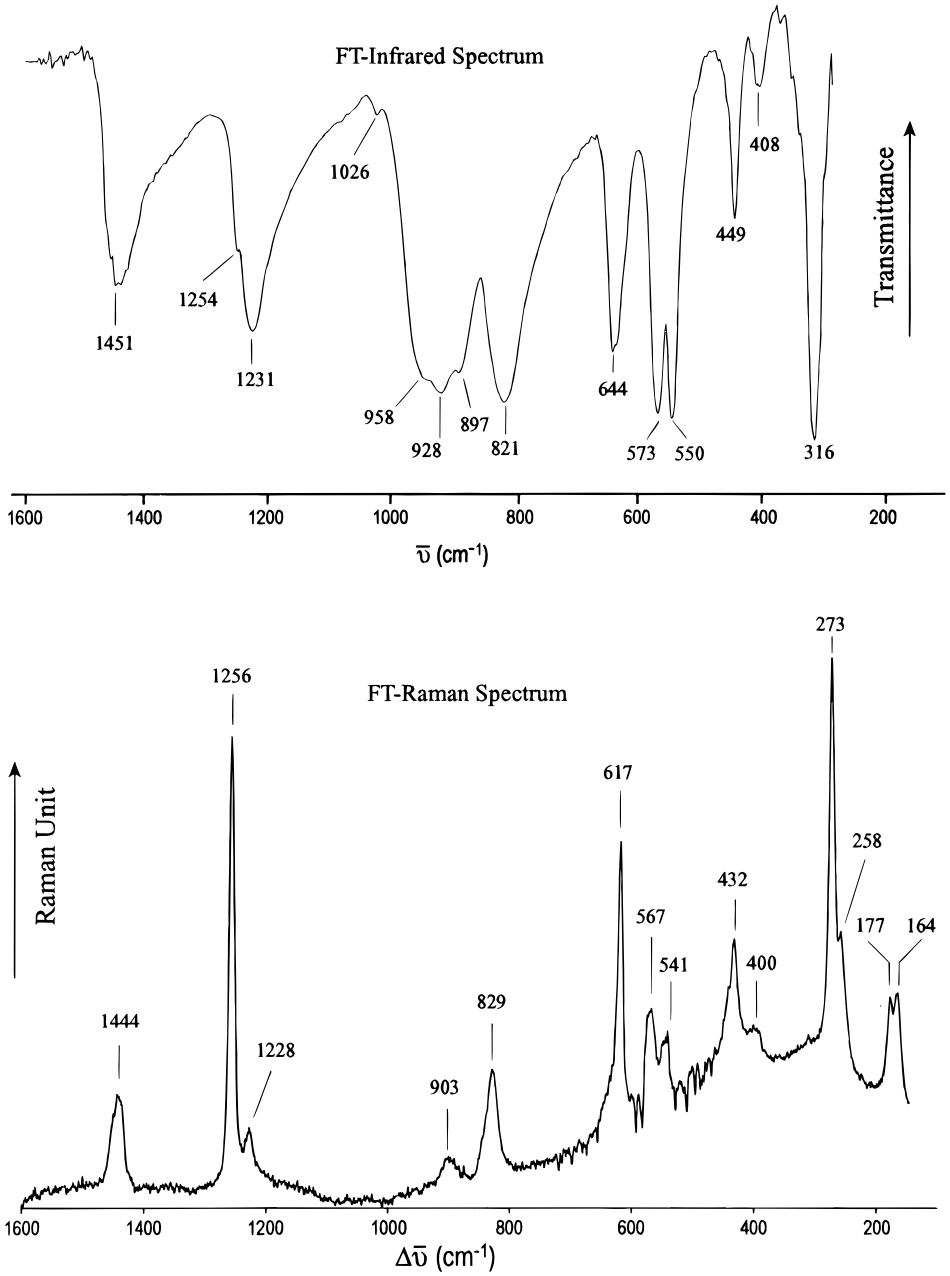

Figure 10. Vibrational spectra of $Cs[Sb(SO_3F)_6]$.

Table 7. Internal Bonding Parameters of the Fluorosulfato Superacid Anions (Bond Lengths in Å; Bond Angles in deg)

molecular anion	M	d(M−O$_b$)[a]	d(S−O$_b$)	∠(MO$_b$S)	d(S−O$_t$)[a]	d(S−F)
$[H(SO_3F)_2]^-$	H^+	1.210(2)	1.471(2)	117.1(2)	1.406(2) 1.399(3)	1.531(2)
$[Au(SO_3F)_4]^-$ [b]	Au^{3+}	1.968(4)	1.508(4)	125.2(3)	1.393(5) 1.402(6)	1.523(6)
$[Pt(SO_3F)_6]^{2-}$	Pt^{4+}	1.987(8)	1.44(1)	135.3(7)	1.48(2) 1.36(1)	1.555(9)
$[Sb(SO_3F)_6]^-$	Sb^{5+}	1.955(2)	1.516(2)	136.6(1)	1.396(3) 1.409(4)	1.486(3)

[a] The subscripts b (bridging) and t (terminal) differentiate between central and peripheral O atoms. [b] The more accurately determined parameters of the group O(1)−S(1)−F(1)−(O(2)-O(3)) are used.

contacts to 3.496(4) Å for O--O separations. Those nonbonded contacts are comparable or slightly larger than the sums of the van der Waal radii,[74] $\sum r_w$, which are 2.94 Å for F--F to 3.04 Å for O--O separations. Hence neither large gaps between peripheral atoms nor steric crowding within the outermost sphere of the $[Sb(SO_3F)_6]^-$ anion are indicated.

The structural analysis for the $[Sb(SO_3F)_6]^-$ anion presented here provides some insights into what appears to be the weakest nucleophile of the superacid anions studied here. It is not surprising that the observed O--Cs contacts (see Table 6) are among the longest and weakest.

Unfortunately data for $[Pt(SO_3F)_6]^{2-}$ are too imprecise for a similar analysis. The remaining two superacid anions are

(74) Bondi, A. *J. Phys. Chem.* **1964**, *68*, 441.

Table 8. Wave Numbers and Relative Intensity of Vibrational Bands (cm^{-1}) for $Cs[Sb(SO_3F)_6]$, $Cs_2[Sn(SO_3F)_6]$, and $Cs_2[Pt(SO_3F)_6]$

$Cs[Sb(SO_3F)_6]$		$Cs_2[Sn(SO_3F)_6]$		$Cs_2[Pt(SO_3F)_6]$		
IR[a]	Raman[a]	IR[a]	Raman[19]	IR[a]	Raman[18]	approx description
1451 s	1444 ms	1399 s	1407 m	1406 vs	1416 w, sh	$\nu_{as}(SO_2)$
			1399 m	1345 vw	1410 m	
1254 vw,sh	1256 vs	1265 w,sh	1270 s	1345 vw	1250 vs	$\nu_{sym}(SO_2)$
1231 s	1228 w, sh	1224 s	1218 w	1213 vs	1219 m	
1026 vw						
958 m, sh	903 w	1088 w,sh	1091 s	1041 w	1043 s	ν(S−O) + ν(S−F)
928 vs		1015 s	995 sh	969 vs	1010 m	
897 m,sh				927 m, sh		
821 vs	829 ms	809 s	828 m	799 s	800 w, b	
			811 m			
644 ms	617 s	632 s	625 s	657 m	634 vs	ν (M−O) + δ (SO_3F)
573 s	567 w	577 ms	578 ms	584 s	579 vw	
550 s	541w	556 ms	560 ms	547 m	550 vw	
449 m	432 m	435 m	431 m	452 w	444 m	
408 w	400 w,sh	410 w	418			
			407 w			
316 s			345 w			
	273 s		260 m		280 vs	τ (MO_n) + τ (SO_3F)
	258 w,sh					
	177 m					
	164 m					

[a] This work.

nonspherical and show linear ($[H(SO_3F)_2]^-$) or square planar ($[Au(SO_3F)_4]^-$) orientation of the outer -SO_2F groups. However as seen in Table 7, S−O_t bond distances for both anions are comparably short, while S−F distances are very slightly longer than in $[Sb(SO_3F)_6]^-$, possibly due to weak F--Cs contacts as discussed.

(c) Vibrational Spectra. The discussion in this section is primarily concerned with the vibrational spectra of $Cs[Sb(SO_3F)_6]$, which have not been reported previously. For $CsSO_3F$,[16c] $Cs[H(SO_3F)_2]$,[17] $Cs[Au(SO_3F)_4]$,[6] and $Cs_2[Pt(SO_3F)_6]$[18] either IR, Raman spectra, or both have been reported before, and an approximate assignment has been made in most instances.[16−18] There are also reports on vibrational spectra of compounds containing either the $[H_3O]^+$ ion[26] or the $[Sb_2F_{11}]^-$ ion.[75−77] For the latter, with bands below 700 cm^{-1}, vibrational spectra are rather uninformative, in particular where the symmetry of the anion is reduced by anion−cation interionic contacts. The complex structure of $[H_3O][Sb_2F_{11}]$ and the reported molecular structure determination make a vibrational analysis both difficult and unnecessary.

We have also commented on the observed small band splittings of E-modes in the IR and Raman spectra of $CsSO_3F$. The cause for these splittings is a slight departure from ideal C_{3v} symmetry for the anion in a monoclinic unit cell, as suggested by the structure, rather than site symmetry effects as suggested earlier[16] where a tetragonal unit cell[31] had been assumed.

The IR and Raman spectra of $Cs[Sb(SO_3F)_6]$ are shown in Figure 10. Table 8 contains the vibrational band positions in cm^{-1} and the relative band intensities for $Cs[Sb(SO_3F)_6]$, $Cs_2[Sn(SO_3F)_6]$,[19] where both anions are isoelectronic, and for $Cs_2[Pt(SO_3F)_6]$.[18]

As expected a similar band distribution is found for all three compounds both in the IR and Raman spectra. This finding is consistent with the presence of monodentate covalent fluorosulfate groups in all three compounds and in agreement with the molecular structures for $Cs[Sb(SO_3F)_6]$ and $Cs_2[Pt(SO_3F)_6]$. In contrast, the vibrational spectra of $Cs[M(SO_3F)_6]$, M = Nb or Ta feature relatively strong bands at 1120 to 1150 cm^{-1}, which have been assigned to bridging fluorosulfate groups.[51] Both salts appear to contain oligomeric anions and both Nb and Ta appear to have coordination numbers higher than six in these compounds.[51] Compared to $Cs[M(SO_3F)_6]$, M = Nb or Ta,[51] and also to $Cs_2[M(SO_3F)_6]$, M = Sn[19] or Pt,[18] the spectra for $Cs[Sb(SO_3F)_6]$ are simpler and band splittings are frequently unresolved. This is consistent with the high symmetry of the $[Sb(SO_3F)_6]^-$ anion. The asymmetric $-SO_2$ stretch at ∼1450 cm^{-1} is about 40−50 cm^{-1} higher than in $[M(SO_3F)_6]^{2-}$, M = Nb or Pt,[51] and reflects strong covalent bonding to the central atom in all SO_3F containing superacid anions.

In view of comparable bond distances for the S−F and S−O_b groups, it appears to be inappropriate to differentiates between S−F and S−O vibrations in $[Sb(SO_3F)_6]^-$, since obviously vibrational mixing occurs. The band separation in this region (∼75 cm^{-1} in the Raman and up to 140 cm^{-1} in the IR spectrum) increases to about 280 cm^{-1} for $Cs_2[Sn(SO_3F)_6]$[19] and about 240 cm^{-1} for $Cs_2[Pt(SO_3F)_6]$.[18]

For all three salts, infrared bands at 620 to about 660 cm^{-1} are observed with Raman bands ∼25 cm^{-1} lower than the corresponding IR bands. We have previously suggested[18,19] that skeletal vibrations of the MO_6 moiety contribute to these bands. It appears that this is also the case for $Cs[Sb(SO_3F)_6]$.

In summary the vibrational spectra obtained for $Cs[Sb(SO_3F)_6]$ and $Cs_2[Pt(SO_3F)_6]$ are consistent with the molecular structures reported here and compare well to vibrational spectra reported for a wide range of salts of the type $Cs_2[M(SO_3F)_6]$, where M = Sn,[19] Ge,[20] Ti,[78] Zr,[78] Hf,[78] Pd,[79] Ir,[80] and Ru.[81] The spectra differ however from vibrational data reported for $Cs[M(SO_3F)_6]$, M = Nb or Ta,[51] where the anion appears to have an oligomeric structure.

(d) Solution Studies in Fluorosulfric Acid. There is limited evidence available that some of the superacid anions which are structurally characterized in the solid state exist also in HSO_3F solution. For $Cs_2[Pt(SO_3F)_6]$ as well as for $Pt(SO_3F)_4$ and the oligomeric salt $Cs[Pt(SO_3F)_5]$ conductometric studies are re-

(75) Gillespie, R. J.; Landa, B. *Inorg. Chem.* **1973**, *12*, 1383.
(76) Bonnet, B.; Mascherpa, G. *Inorg. Chem.* **1980**, *19*, 785.
(77) Craig, N. C.; Fleming, G. F.; Panata, J. *J. Am. Chem. Soc.* **1985**, *107*, 7324.
(78) Mistry, F.; Aubke, F. *J. Fluorine Chem.* **1994**, *68*, 239.
(79) (a) Lee, K. C.; Aubke, F. *Can. J. Chem.* **1977**, *55*, 2473. (b) Lee, K. C.; Aubke, F. *Can. J. Chem.* **1979**, *57*, 2058.
(80) Lee, K. C.; Aubke F. *J. Fluor. Chem.* **1982**, *19*, 501.
(81) Leung, P. C.; Aubke F. *Can. J. Chem.* **1985**, *62*, 2892.

ported[18] and $Cs_2[Pt(SO_3F)_6]$ is found to behave as a weak base as expected. Additional evidence comes from UV and Raman spectra in solution, even though in the latter case extensive overlap with solvent bands allows the (unambiguous) identification of a limited number of bands only.

Likewise in the conjugate superacid $HSO_3F-Au(SO_3F)_3$[6] electronic spectra and conductometry for $Au(SO_3F)_3$ and $K[Au(SO_3F)_4]$ are reported.[6a] Again the reported Raman spectrum of $Cs[Au(SO_3F)_4]$ in HSO_3F is of limited use on account of extensive overlap with solvent bands.[6a]

More conclusive are ^{19}F-NMR studies in fluorosulfuric acid. Single line resonances, well separated from the solvent single line, are observed for $Cs[Sb(SO_3F)_6]$ at 46.36 ppm (vs solvent at 40.86 ppm), for $Cs[Au(SO_3F)_4]$ at 45.50 ppm (vs solvent at 40.80 ppm)[6] and $Cs_2[Pt(SO_3F)_6]$ at 47.75 ppm (vs solvent at 40.70 ppm).[18] In the latter case, satellite peaks due to coupling to ^{195}Pt are observed with $J_1 = 31$ Hz, but it has not been possible to obtain a ^{195}Pt-NMR spectrum.[18] This in turn suggests that the three superacid anions $[Sb(SO_3F)_6]^-$, $[Pt(SO_3F)_6]^{2-}$, and $[Au(SO_3F)_4]^-$ exist at ambient temperature in HSO_3F as detectable, presumably solvated species and have symmetrical structures giving rise to a single ^{19}F resonances. It can be concluded that rapid SO_3F^- exchange with the solvent (HSO_3F) does not occur.

For solutions of $CsSO_3F$ or of $Cs[H(SO_3F)_2]$ in HSO_3F only a single sharp line is observed in the ^{19}F-NMR spectrum, which suggests a rapid equilibrum of the type

$$SO_3F^- + HSO_3F \overset{HSO_3F}{\rightleftharpoons} [H(SO_3F)_2]^- \qquad (10)$$

Finally the anion $[Sb_2F_{11}]^-$ has been identified previously in the ^{19}F-NMR spectrum of magic acid[23-25] where it is found at SbF_5 concentrations above 30 mol % as a minor constituent.

Summary and Conclusions

This study has involved the structural characterization of six salts containing superacid anions with Cs^+ as cation in five instances. The anions are all formally derived from protonic superacid systems by proton transfer. The anions SO_3F^- and $[H(SO_3F)_2]^-$ form in the Brönsted acid fluorosulfuric acid, while the homoleptic conjugate superacid systems $HSO_3F-Au(SO_3F)_3$,[6] $HSO_3F-Pt(SO_3F)_4$,[18] and $HSO_3F-Sb(SO_3F)_5$, which still needs to be fully developed and explored, give rise to the anions $[Au(SO_3F)_4]^-$, $[Pt(SO_3F)_6]^{2-}$, and $[Sb(SO_3F)_6]^-$.

To the five Cs^+ salts is added the oxonium salt $[H_3O][Sb_2F_{11}]$, which is unexpectedly isolated from magic acid, HSO_3F-SbF_5. The anion, $[Sb_2F_{11}]^-$ is formally derived from the very strong[1-3] superacid $HF-SbF_5$.

The structural characterization of the six anions allows two general conclusions: (i) The very low nucleophilicity of the anions is apparent from very strong covalent bonds within the anions, in particular to peripheral hard O and F atoms. (ii) Weak secondary interionic contacts of the superacid anions involve primarily oxygen and to a lesser degree fluorine as donor atom. Such secondary interactions are found to be very important in stabilizing unusual, highly electrophilic molecular cations, such as the linear $[Hg(CO)_2]^{2+}$ cation found in $[Hg(CO)_2][Sb_2F_{11}]_2$,[40] the first post-transition metal carbonyl derivative. Both properties, the very low nucleophilicity of superacid anions and their ability to engage in long range hard acid−hard base interactions between electrophilic centers in highly reactive molecular cations and hard, tightly bonded peripheral O and F atoms of the anion, are in our view essential in endeavors to stabilize unusual cations in the solid state or in superacidic solution. The second aspect had not been fully recognized and appreciated previously. The quest for large, bulky anions with low ionic charges to act as "noncoordinating" or later as "least coordinating anions"[37,82] becomes at best a laudable, but rather pointless academic exercise. A lack of or a substantial reduction in the coordinating ability of anions via secondary bonds is neither realistic in organometallic complexes[83] nor in our view desirable.

Acknowledgment. Financial support by the Natural Science and Engineering Research Council of Canada (NSERC) is gratefully acknowledged. The Alexander von Humboldt Foundation is thanked for the granting of a Research Award to F.A. The North Atlantic Treaty Organization NATO is thanked for a Collaborative Research Grant (to F.A. et al.). We thank Professors Hägele (Universität Düsseldorf) and Willner (Universität Hannover) for helpful discussions.

Supporting Information Available: A complete table of crystallographic data, atomic coordinates, anisotropic thermal parameters, bond distances and angles, torsion angles, and intermolecular contacts for the six structures (58 pages). Ordering information is given on any current masthead page.

IC960525L

(82) Rosenthal, M. R. *J. Chem. Educ.* **1973**, *50*, 331.
(83) Beck, W.; Sünkel, K. *Chem. Ber. Rev.* **1988**, *88*, 1405.